



HAL
open science

DOCK11 deficiency in patients with X-linked actinopathy and autoimmunity

Charlotte Boussard, Laure Delage, Tania Gajardo, Alexandre Kauskot, Maxime Batignes, Nicolas Goudin, Marie-Claude Stolzenberg, Camille Brunaud, Patricia Panikulam, Quentin Riller, et al.

► **To cite this version:**

Charlotte Boussard, Laure Delage, Tania Gajardo, Alexandre Kauskot, Maxime Batignes, et al.. DOCK11 deficiency in patients with X-linked actinopathy and autoimmunity. *Blood*, 2023. hal-04246983

HAL Id: hal-04246983

<https://hal.science/hal-04246983v1>

Submitted on 18 Oct 2023

HAL is a multi-disciplinary open access archive for the deposit and dissemination of scientific research documents, whether they are published or not. The documents may come from teaching and research institutions in France or abroad, or from public or private research centers.

L'archive ouverte pluridisciplinaire **HAL**, est destinée au dépôt et à la diffusion de documents scientifiques de niveau recherche, publiés ou non, émanant des établissements d'enseignement et de recherche français ou étrangers, des laboratoires publics ou privés.



American Society of Hematology
2021 L Street NW, Suite 900,
Washington, DC 20036
Phone: 202-776-0544 | Fax 202-776-0545
editorial@hematology.org

DOCK11 deficiency in patients with X-linked actinopathy and autoimmunity

Tracking no: BLD-2022-018486R1

Charlotte Boussard (Hospital Necker-Enfants Malades, Assistance Publique-Hospitaux de Paris, INSERM, France) Laure Delage (Université Paris Cité, Institut Imagine, Laboratory of Immunogenetics of Pediatric Autoimmune Diseases, INSERM UMR 1163; F-75015 Paris, France., France) Tania Gajardo (INSERM U1163 - Imagine Institute, France) Alexandre Kauskot (INSERM, France) Maxime Batignes (Institut Imagine-INSERM-UMR-1163, France) Nicolas GOUDIN (INSERM, France) Marie-Claude Stolzenberg (U768, France) Camille Brunaud (Imagine Institute, France) Patricia Panikulam (INSERM U1163 - Imagine Institute, France) Quentin Riller (Université Paris Cité, Institut Imagine, Laboratory of Immunogenetics of Pediatric Autoimmune Diseases, INSERM UMR 1163; F-75015 Paris, France., France) Maryse Moya-Nilges (Institut Pasteur, UTechS Ultrastructural BioImaging UBI, France) Jean Solarz (INSERM, France) Christelle REPERANT (INSERM, France) Béatrice Durel (Cell Imaging Platform, Structure Fédérative de Recherche Necker, INSERM US24, CNRS UMS3633, France) Jean-Claude Bordet (Hospices civils de Lyon, France) Olivier Pellé (Université Paris Cité, Institut Imagine, Laboratory of Immunogenetics of Pediatric Autoimmune Diseases, INSERM UMR 1163; F-75015 Paris, France, France) Corinne Lebreton (Institut Imagine-INSERM-UMR-1163, France) Aude Magerus-Chatinet (INSERM, France) Vithura Pirabakaran (Université Paris Cité, Institut Imagine, Laboratory of Immunogenetics of Pediatric Autoimmune Diseases, INSERM UMR 1163; F-75015 Paris, France., France) Pablo Vargas (INSERM, France) Sébastien Dupichaud (Cell Imaging Platform, Structure Fédérative de Recherche Necker, INSERM US24, CNRS UMS3633, France) Marie Jeanpierre (Institut Imagine-INSERM-UMR-1163, France) Angélique Vinit (Sorbonne Université, France) Mohammed Zarhrate (Imagine Institute,) Cécile Masson (Bioinformatics Platform, Imagine Institute, INSERM UMR1163, Paris Cité University, Paris, France., France) Nathalie Aladjidi (Bordeaux University Hospital / CEREVANCE, France) Peter Arkwright (University of Manchester, United Kingdom) Brigitte Bader-Meunier (AP-HP5, France) Sandrine Baron Joly (Department of Pediatrics, Nîmes University Hospital, France) Joy Benadiba (Nice University Hospital, France) Elise Bernard (Departement of General Pediatrics, Centre hospitalier de Mayotte, France) Dominique Berrebi (Hopital Robert Debré, APHP,) Christine Bodemer (Hôpital Necker-Enfants Malades, France) Martin CASTELLE (Hôpital Universitaire Necker Enfants Malades, France) Fabienne Charbit-Henrion (Department of Dermatology, referral Center for Genodermatoses (MAGEC), Assistance Publique-Hopitaux de Paris, Hôpital Necker-Enfants Malades, F-75015, Paris, France., France) Marwa Chbihi (INSERM U976 HIPI, équipe INSIGHT, Institut de Recherche Saint Louis, Université Paris Cité, Paris, France, France) Agathe Debray (Departement of General Pediatrics and Infectious Diseases, Hôpital Trousseau, Assistance Publique-Hôpitaux de Paris, France) Philippe Drabent (Department of Anatomopathology, Assistance Publique-Hopitaux de Paris, Hôpital Necker-Enfants Malades, France) Sylvie Fraitag (Hôpital Necker-Enfants Malades, France) Miguel Hié (APHP, CHU la Pitié-Salpêtrière, France) Judith Landman-Parker (Armand-Trousseau Sorbonne University Hospital, AP-HP, France) Ludovic Lhermitte (Assistance Publique-Hôpitaux de Paris (AP-HP), Hôpital Necker Enfants-Malades, Paris, France, France) Despina Moshous (Hôpital Necker-Enfants Malades, France) Pierre Rohrllich (CHU de Nice, France) Frank Ruummele (Department of Pediatric Gastroenterology, Assistance Publique-Hopitaux de Paris, Hôpital Necker-Enfants Malades, France) Anne Welfringer-Morin (Department of Dermatology, referral Center for Genodermatoses (MAGEC), Assistance Publique-Hopitaux de Paris, Hôpital Necker-Enfants Malades, France) Maud Tusseau (The International Center of Research in Infectiology, Lyon University, INSERM U1111, CNRS UMR 5308, ENS, UCBL, France) Alexandre Belot (HCL, INSERM, Université de Lyon,) Nadine Cerf-Bensussan (INSERM, France) Marie Roelens (Necker Hospital, France) Capucine Picard (Université de Paris, France) Bénédicte Neven (Hospital Necker-Enfants Malades, Assistance Publique-Hospitaux de Paris, INSERM, France) Alain Fischer (INSTITUT IMAGINE, France) Isabelle Callebaut (Sorbonne University, CNRS UMR7590, Museum National d'Histoire Naturelle, France) Mickaël Ménager (Université Paris Cité, Institut Imagine, Laboratory of Inflammatory Responses and Transcriptomic Networks in Diseases, Atip-Avenir Team, INSERM UMR 1163; F-75015 Paris, France., France) Fernando Sepulveda (INSERM U1163 - Imagine Institute, France) Frédéric Adam (INSERM, France) Frédéric Rieux-Laucat (Institut Imagine-INSERM-UMR-1163, France)

Abstract:

Dedicator of cytokinesis (DOCK) proteins play a central role in actin cytoskeleton regulation. This is highlighted by the DOCK2 and DOCK8 deficiencies leading to actinopathies and immune deficiencies. DOCK8 and DOCK11 activate CDC42, a RHO-GTPase involved in actin cytoskeleton dynamics, among many cellular functions. The role of DOCK11 in human immune disease has been long suspected but has never been described so far. We studied eight male patients, from seven unrelated families, with hemizygous *DOCK11* missense variants leading to reduced DOCK11 expression. The patients were presenting with early-onset autoimmunity, including cytopenia, systemic lupus erythematosus, skin, and digestive manifestations. Patients' platelets exhibited abnormal ultrastructural morphology and spreading as well as impaired CDC42 activity. *In vitro* activated T cells and B lymphoblastoid cell lines (B-LCL) of patients exhibited aberrant protrusions and abnormal migration speed in confined channels concomitant with altered actin polymerization during migration. A DOCK11 knock-down recapitulated these abnormal cellular phenotypes in monocytes-derived dendritic cells (MDDC) and primary activated T cells from healthy controls. Lastly, in line with the patients' autoimmune manifestations, we also observed abnormal regulatory T cells (Tregs) phenotype with profoundly reduced FOXP3 and IKZF2 expression. Moreover, we found a reduced T cell proliferation and an impaired STAT5B phosphorylation upon IL2 stimulation of the patients' lymphocytes. In conclusion, DOCK11 deficiency is a new X-linked immune-related actinopathy leading to impaired CDC42 activity and STAT5 activation, and associated with abnormal actin cytoskeleton remodeling as well as Tregs phenotype culminating in immune dysregulation and severe early-onset autoimmunity.

Conflict of interest: COI declared - see note

COI notes: L.D. is a former employee of Sanofi, France and may hold shares and/or stock options in the company. Other authors have nothing to disclose.

Preprint server: No;

Author contributions and disclosures: Conceptualization, C.B., L.D., T.G., A.F., A.K., F.A., F.E.S., I.C., F.R-L.; Methodology, I.C., P.V.; Investigation, C.B., LD., T.G., A.K., M.B., C.Bru., B.D., M.M.-N., J.S., C.R., J-C.B., P.P., M-C.S., O.P., A.M., V.P., P.V., S.B., A.V., M.Z., C.M., M.R.; Data Curation, L.D., N.G., I.C., Q.R., C.M.; Formal Analysis, C.B., L.D., I.C., T.G., P.P., Q.R.; Writing - Original Draft, C.B., L.D., T.G., F.E.S., I.C., A.K., F.A., F.R-L.; Writing, Review & Editing, I.C., Q.R., N.A., P.D.A., M.C., N.C-B., F.C-H., S.F., P.D., L.L., D.M., P.R., P.P., A.W-M., M.R., B.N., J-C.B., A.M., A.K., F.A., M.B., M-C.S., C.B., L.D., F.R-L.; Visualization, I.C., L.D., C.B., Q.R., N.G., T.G., P.P., F.A., A.K., M.M-N, B.D., J-C.B., T.G.; Resources, C.L., N.A., P.D.A., B.B-M., S.B-J., A.B., J.B., E.B., D.B., C.Bod., M.C., N.C-B., F.C-H., A.D., S.F., P.D., M.H., J.L-P., L.L., M.J., P.R., F.R., M.T., A.W-M., M.R., C.P., B.N.; Supervision, M.M., F.E.S., A.K., F.A., F.R-L.; Funding Acquisition, F.E.S., F.R-L. All authors reviewed the manuscript.

Non-author contributions and disclosures: No;

Agreement to Share Publication-Related Data and Data Sharing Statement: For original data, please contact frederic.rioux-laucat@inserm.fr. A statement "Data are available upon request to the corresponding author" has been added in the Methods section.

Clinical trial registration information (if any):

1 **Title: DOCK11 deficiency in patients with X-linked actinopathy and autoimmunity**

2
3 **Authors:**

4 Charlotte Boussard,^{1,*} Laure Delage,^{1,*} Tania Gajardo,^{2,†} Alexandre Kauskot,^{3,†} Maxime
5 Batignes,^{4,†} Nicolas Goudin,⁵ Marie-Claude Stolzenberg,¹ Camille Brunaud,¹ Patricia
6 Panikulam,² Quentin Riller,¹ Maryse Moya-Nilges,⁶ Jean Solarz,³ Christelle Repérant,³
7 Béatrice Durel,⁷ Jean-Claude Bordet,⁸ Olivier Pellé,^{1,9} Corinne Lebreton,¹⁰ Aude Magérus,¹
8 Vithura Pirabakaran,¹ Pablo Vargas,¹¹ Sébastien Dupichaud,⁶ Marie Jeanpierre,¹ Angélique
9 Vinit,¹² Mohammed Zarhrate,¹³ Cécile Masson,¹⁴ Nathalie Aladjidi,^{15, 16} Peter D. Arkwright,¹⁷
10 Brigitte Bader-Meunier,^{1, 18} Sandrine Baron Joly,¹⁹ Joy Benadiba,²⁰ Elise Bernard,²¹
11 Dominique Berrebi,²² Christine Bodemer,²³ Martin Castelle,¹⁸ Fabienne Charbit-
12 Henrion,^{10,24,25} Marwa Chbihi,¹⁸ Agathe Debray,²⁶ Philippe Drabent,²⁷ Sylvie Fraitag,²⁷
13 Miguel Hié,²⁸ Judith Landmann-Parker,²⁹ Ludovic Lhermitte,³⁰ Despina Moshous,^{18, 31, 32}
14 Pierre Rohrllich,²⁰ Frank Ruemmele,²⁴ Anne Welfringer-Morin,²³ Maud Tusseau,³³ Alexandre
15 Belot,^{33,34,35} Nadine Cerf-Bensussan,¹⁰ Marie Roelens,^{36,37} Capucine Picard,^{32,37,38} Bénédicte
16 Neven,^{1, 18} Alain Fischer,^{38, 39, 40} Isabelle Callebaut,⁴¹ Mickaël Ménager,^{4,42, ‡} Fernando E.
17 Sepulveda,^{2,‡} Frédéric Adam,^{3,‡} Frédéric Rieux-Laucat,^{1,‡}.

18
19 * Dr. Charlotte Boussard and Dr. Laure Delage contributed equally to this work.

20 † Dr. Gajardo, Dr. Kauskot, and Dr. Batignes contributed equally to this work.

21 ‡ Dr. Ménager, Dr. Sepulveda, Dr. Adam, and Dr. Rieux-Laucat share senior authorship.

22
23 **Affiliations:**

24 ¹Université Paris Cité, Institut Imagine, Laboratory of Immunogenetics of Pediatric
25 Autoimmune Diseases, INSERM UMR 1163; F-75015 Paris, France.

26
27 ²Université Paris Cité, Institut Imagine, Laboratory of Molecular Basis of Altered Immune
28 Homeostasis, INSERM UMR 1163; F-75015 Paris, France.

29
30 ³INSERM, UMR_S1176, Université Paris-Saclay, F- 94276 Le Kremlin-Bicêtre, France.

31
32 ⁴Université Paris Cité, Institut Imagine, Laboratory of Inflammatory Responses and
33 Transcriptomic Networks in Diseases, Atip-Avenir Team, INSERM UMR 1163; F-75015
34 Paris, France.

35
36 ⁵Necker Bio-image Analysis Platform, Structure Fédérative de Recherche Necker, INSERM
37 US24, CNRS UMS3633, F-75015 Paris, France.

38
39 ⁶Institut Pasteur, UTechS Ultrastructural BioImaging UBI, F-75015 Paris, France.

40 x

41 ⁷Cell Imaging Platform, Structure Fédérative de Recherche Necker, INSERM US24, CNRS
42 UMS3633, F-75015 Paris, France.

43
44

45 ⁸Laboratoire d'Hémostase, Centre de Biologie Est, Hospices Civils de Lyon, F-68500 Bron,
46 France.
47

48 ⁹Flow Cytometry Core Facility, Structure Fédérative de Recherche Necker INSERM US24,
49 CNRS UMS3633, F-75015 Paris, France.
50

51 ¹⁰Université Paris Cité, Imagine Institute, Laboratory of Intestinal Immunity, INSERM UMR
52 1163; F-75015 Paris, France.
53

54 ¹¹Institut Necker Enfants Malades (INEM), INSERM U1151/CNRS UMR 8253, Université
55 de Paris, 156-160 rue de Vaugirard, 75015 Paris, France.
56

57 ¹²Sorbonne Université, UMS037, PASS, Plateforme de cytométrie de la Pitié-Salpêtrière
58 CyPS; F-75013 Paris, France.
59

60 ¹³Genomics Core Facility, Institut Imagine-Structure Fédérative de Recherche Necker,
61 INSERM U1163 et INSERM US24/CNRS UAR3633, Université Paris Cite ; F-75015 Paris,
62 France.
63

64 ¹⁴Bioinformatics Core Facility, Institut Imagine-Structure Fédérative de Recherche Necker,
65 INSERM U1163 et INSERM US24/CNRS UAR3633, Paris Cite University, Paris, France
66

67 ¹⁵Centre de Référence National des Cytopénies Auto-immunes de l'Enfant (CEREVANCE),
68 Bordeaux, France.
69

70 ¹⁶Pediatric Oncology Hematology Unit, University Hospital, Plurithématique CIC (CICP),
71 Centre d'Investigation Clinique (CIC) 1401, INSERM, Bordeaux, France.
72

73 ¹⁷Lydia Becker Institute of Immunology and Inflammation, University of Manchester &
74 Department of Pediatric Allergy and Immunology, Royal Manchester Children's Hospital,
75 Oxford Road, Manchester, UK.
76

77 ¹⁸Pediatric Immunology, Hematology and Rheumatology Department, Hôpital Necker-
78 Enfants Malades, Assistance Publique-Hôpitaux de Paris (AP-HP); F-75015 Paris, France.
79

80 ¹⁹Department of Pediatrics, Nîmes University Hospital, Nîmes, France.
81

82 ²⁰Department of Pediatric Hematology-Oncology, Nice University Hospital, Nice, France.
83

84 ²¹Departement of General Pediatrics, Centre hospitalier de Mayotte, Mamoudzou, Mayotte,
85 France.
86

87 ²²Department of Pediatric Pathology, Hôpital Robert-Debré, Hôpital Universitaire Robert-
88 Debré, Assistance Publique-Hôpitaux de Paris, Paris, France.

89
90 ²³Department of Dermatology, referral Center for Genodermatoses (MAGEC), Assistance
91 Publique-Hopitaux de Paris, Hôpital Necker–Enfants Malades, F-75015, Paris, France.
92
93 ²⁴Department of Pediatric Gastroenterology, Assistance Publique-Hopitaux de Paris, Hôpital
94 Necker–Enfants Malades, F-75015, Paris, France.
95
96 ²⁵Department of Genomic Medicine for Rare Diseases, Assistance Publique-Hopitaux de
97 Paris, Hopital Necker–Enfants Malades, F-75015, Paris, France.
98
99 ²⁶Departement of General Pediatrics and Infectious Diseases, Hôpital Trousseau, Assistance
100 Publique-Hôpitaux de Paris, Paris, France.
101
102 ²⁷Department of Anatomopathology, Assistance Publique-Hopitaux de Paris, Hôpital Necker–
103 Enfants Malades, F-75015, Paris, France.
104
105 ²⁸Sorbonne Université, Assistance Publique - Hôpitaux de Paris, Groupement Hospitalier
106 Pitié-Salpêtrière, Service de Médecine Interne 2, Institut E3M, Inserm UMRS 1135, Centre
107 d’Immunologie et des Maladies Infectieuses (CIMI-Paris), Paris, France.
108
109 ²⁹Sorbonne Université, Pediatric Hematology Oncology department, Hôpital Armand-
110 Trousseau, AP-HP, F-75012-Paris, France.
111
112 ³⁰Laboratory of Onco-Haematology, AP-HP, Université de Paris Cité, Institut Necker-Enfants
113 Malades, INSERM UMR 1151, F-75015, Paris, France
114
115 ³¹Université Paris Cité, Imagine Institute, Laboratory of Genome Dynamics in the Immune
116 System, INSERM UMR 1163, F-75015 Paris, France.
117
118 ³²French National Reference Center for Primary Immune Deficiencies (CEREDIH), Necker-
119 Enfants Malades University Hospital, AP-HP; F-75015 Paris, France.
120
121 ³³The International Center of Research in Infectiology, Lyon University, INSERM U1111,
122 CNRS UMR 5308, ENS, UCBL, Lyon, France.
123
124 ³⁴National Referee Centre for Rheumatic and Autoimmune Diseases in Children, RAISE,
125 Paris and Lyon, France.
126
127 ³⁵Pediatric Nephrology, Rheumatology, Dermatology Department, Hôpital Femme Mère
128 Enfant, Hospices Civils de Lyon, 59 Bd Pinel, 68677, Bron Cedex, France.
129
130 ³⁶Université Paris Cité, Paris, France.
131

132 ³⁷Study Center for Primary Immunodeficiencies (CEDI), Hôpital Necker-Enfants Malades
133 University, AP-HP; F-75015 Paris, France.

134

135 ³⁸Université Paris Cité, Imagine Institute, INSERM UMR 1163; F-75015 Paris, France

136

137 ³⁹Department of Pediatric Immuno-Haematology and Rheumatology, Reference Center for
138 Rheumatic, AutoImmune and Systemic Diseases in Children (RAISE), Hôpital Necker-
139 Enfants Malades, Assistance Publique – Hôpitaux de Paris (AP-HP); F-75015 Paris, France.

140

141 ⁴⁰Collège de France ; F-75231 Paris, France.

142

143 ⁴¹Sorbonne Université, Muséum National d'Histoire Naturelle, CNRS UMR 7590, Institut de
144 Minéralogie, de Physique des Matériaux et de Cosmochimie, F-75005 Paris, France.

145

146 ⁴²Labtech Single-Cell@Imagine, Imagine Institute, INSERM UMR 1163; F-75015 Paris,
147 France.

148

149 **Corresponding author:**

150 Dr Frédéric Rieux-Laucat, Institut *Imagine*, 24 Boulevard du Montparnasse, 75015, Paris,
151 France ; Email: frederic.rioux-laucat@inserm.fr.

152 **ABSTRACT**

153

154 Deducator of cytokinesis (DOCK) proteins play a central role in actin cytoskeleton regulation.
155 This is highlighted by the DOCK2 and DOCK8 deficiencies leading to actinopathies and
156 immune deficiencies. DOCK8 and DOCK11 activate CDC42, a RHO-GTPase involved in
157 actin cytoskeleton dynamics, among many cellular functions. The role of DOCK11 in human
158 immune disease has been long suspected but has never been described so far. We studied
159 eight male patients, from seven unrelated families, with hemizygous *DOCK11* missense
160 variants leading to reduced DOCK11 expression. The patients were presenting with early-
161 onset autoimmunity, including cytopenia, systemic lupus erythematosus, skin, and digestive
162 manifestations. Patients' platelets exhibited abnormal ultrastructural morphology and
163 spreading as well as impaired CDC42 activity. *In vitro* activated T cells and B lymphoblastoid
164 cell lines (B-LCL) of patients exhibited aberrant protrusions and abnormal migration speed in
165 confined channels concomitant with altered actin polymerization during migration. [A](#)
166 [DOCK11 knock-down recapitulated these abnormal cellular phenotypes in monocytes-](#)
167 [derived dendritic cells \(MDDC\) and primary activated T cells from healthy controls. Lastly,](#)
168 [in line with the patients' autoimmune manifestations, we also observed abnormal regulatory T](#)
169 [cells \(Tregs\) phenotype with profoundly reduced FOXP3 and IKZF2 expression. Moreover,](#)
170 [we found a reduced T cell proliferation and an impaired STAT5B phosphorylation upon IL2](#)
171 [stimulation of the patients' lymphocytes. In conclusion, DOCK11 deficiency is a new X-](#)
172 [linked immune-related actinopathy leading to impaired CDC42 activity and STAT5](#)
173 [activation, and associated with abnormal actin cytoskeleton remodeling as well as Tregs](#)
174 [phenotype culminating in immune dysregulation and severe early-onset autoimmunity.](#)

175

176 **Running title:** DOCK11 actinopathy associated with autoimmunity

177

178 **Key points:**

- 179 • DOCK11 deficiency is a new X-linked immune-related actinopathy.
180
181 • DOCK11 deficiency leads to impaired CDC42 activity, abnormal actin cytoskeleton
182 remodeling, and immune dysregulation.

183

184 Word count: 4096, Abstract word count: 245, Figures/Tables: 6/1, Number of references: 45.

185

186 **Introduction**

187 Immune-related actinopathies are inborn errors of immunity (IEIs) due to gene defects
188 impacting actin cytoskeleton remodeling. More than 20 entities are described so far¹. Actin
189 cytoskeleton remodeling is a dynamic and tightly regulated process crucial for cell shape
190 modifications, cell adhesion, motility, and other main cellular functions². Rho-GTPases, RAS-
191 related GTP-binding proteins, such as RAC, CDC42, and RHO, are key players in the
192 intracellular actin reorganization^{3,4}. The phenotypic spectrum of *RAC2* mutations ranges from
193 granulocytes deficiency (loss-of-function mutations) to SCID with bone-marrow hypoplasia
194 (gain-of-function mutations)⁵. *De novo* mutations in *CDC42* were recently found in patients

195 presenting with Takenouchi-Kosaki syndrome, associating features such as
196 macrothrombocytopenia and developmental abnormalities, or with neo-natal cytopenia with
197 dyshematopoiesis, autoinflammation, rash and hemophagocytic lymphohistiocytosis (HLH),
198 termed NORCAH syndrome⁶. Rho-GTPases are activated by Guanine Exchange Factors
199 (GEFs), such as dedicator of cytokinesis (DOCK) family members like DOCK2 and
200 DOCK8⁷. Biallelic mutations in *DOCK2* result in early-onset invasive bacterial and severe
201 viral infections and T cell lymphopenia⁸. *DOCK8* mutations also result in severe bacterial,
202 viral, and fungal infections, as well as eczema and severe environmental allergies⁹. These
203 descriptions highlight the predominant role of DOCK protein members in immune-related
204 actinopathies¹⁰. A role of DOCK11 in human immune disease has been long suspected but
205 never described so far. Here we identified seven hemizygous mutations in *DOCK11*, a
206 member of the DOCK-D subfamily, in eight patients with early-onset autoimmunity,
207 including autoimmune cytopenia and systemic lupus erythematosus (SLE).

208 **Methods**

209 This section briefly describes the methods; further details are provided in the supplemental
210 Appendix. Before the study, all patients signed informed consents approved by the CERAPH-
211 Centre (IRB: #00011928). The biological samples are part of Inserm UMR1163/Imagine
212 collection declared to the French Ministère de la recherche (CODECOH n° DC-2020-3994).

213

214 **Protein structure analysis**

215 3D structure prediction of DOCK11 protein was performed by combining information from
216 literature-described structures and AlphaFold2 predictions¹¹. The detailed method is described
217 in the supplemental appendix.

218

219 **Genetic and functional analysis**

220 Whole exome (WES) and Sanger sequencing, mass cytometry, ELISA and G-LISA, confocal
221 microscopy, migration assays, and *DOCK11* knock-down methods are detailed in the
222 supplemental appendix.

223

224 **Statistical analysis**

225 Statistical analyses were performed using GraphPad Prism6 (GraphPad, La Jolla, CA, USA).
226 Data were analyzed by one-way ANOVA followed by a post-hoc test, or unpaired non-
227 parametric Mann-Whitney tests or Kruskal-Wallis' tests as indicated in the figure legends.
228 Differences were considered significant when $p < 0.05$.

229

230 **Data sharing statement**

231 [For original data, please contact frederic.rioux-laucat@inserm.fr.](mailto:frederic.rioux-laucat@inserm.fr)

232

233 **Results**

234

235 **Clinical and biological features of the cohort**

236 Eight male patients (7 to 29 years of age) from seven families of various ethnic origins were
237 studied. Clinical and biological data are summarized in Table 1, Table S1, and Fig. S1.
238 Detailed clinical cases are in the Supplemental appendix.

239 All patients presented early-onset autoimmunity at a median age of 5 years (range, 1 to 14
240 years). Five patients (A, C, E, F, G) had autoimmune cytopenia (Table 1). Twin patients (D1
241 and D2) had systemic lupus erythematosus (SLE). Patient B had a severe Rheumatoid Factor
242 (RF) positive polyarticular juvenile arthritis and recurrent hemolytic anemia with positive
243 Coombs tests. In addition, patient F had an auto-inflammatory syndrome with
244 lymphoproliferation (Suppl. Appendix).

245 Five patients (A, C, D1, D2, F) presented with various cutaneous manifestations (detailed in
246 Table1, Fig.1A, and S1), and four patients (A, B, D1, F) with digestive manifestations (Table
247 1 and Fig. S2). None of the patients presented with recurrent or severe infections, allergies **nor**
248 **bleeding disorders**.

249 Among the maternal carriers, patient B's mother had metastatic melanoma and has been
250 treated with immunotherapy; patient C's mother died of colorectal cancer at age 52.

251

252 **Hemizygous deleterious mutations in *DOCK11***

253 Seven different hemizygous **missense variants** of *DOCK11* were identified by Whole-exome
254 sequencing (WES) (Fig. 1B) in seven unrelated and non-consanguineous families. All six
255 mothers tested carried the gene variants (Fig. S3A). **We assessed the expression of the mutant**
256 **and wild-type alleles in CD4⁺, and CD8⁺ T cells, B cells and monocytes in two mothers. The**
257 **expression of both DOCK11 alleles was similar, indicating a global random X-inactivation in**
258 **T and B cells as well as in monocytes (Fig S3B).** These mutations were predicted to be
259 deleterious *in silico*, and five are private variants (Fig. S3A). The mutated amino-acids are
260 located in distinct domains of the DOCK11 protein (Fig 1B). Prediction of DOCK11 protein
261 3D structure allowed to apprehend mutations' potential deleterious impact (Fig. 1C-D and
262 Fig. S4) and suggests that the variants may cause abnormal protein folding or directly impact
263 DOCK11 interactions with its partners. Finally, DOCK11 expression was **variably** reduced in
264 lysates from patients' activated T cells (Fig. 1E).

265

266 ***DOCK11* mutations impair platelets functions and morphology**

267 Platelets play a central role in ITP and participate in the immune dysregulation in SLE
268 pathogenesis¹². As four patients presented with immune thrombocytopenia (ITP) and two
269 patients with SLE, we investigated the impact of *DOCK11* mutations on platelet functions.

270 **A significant decrease in the expression of DOCK11 was observed in the patients' platelets**
271 **compared to healthy donors (Fig. 2A).**

272 Patients' platelet counts were normal or subnormal, except for patients A and C, who
273 presented mild to severe thrombocytopenia (Fig. 2B) but without glycosylation profile defect
274 (Fig. S5A). Platelet size was also normal for the patients, except for patient A who exhibited
275 macroplatelets (Fig. 2C and Fig.S5B). Moreover, electron microscopy ultrastructure analysis
276 revealed abnormal morphology with elongated platelets in patients D1, D2, and G, contrasting
277 with the discoid shape of resting platelets in healthy donors (HDs) (Fig. 2D-F).

278 Five, out of six patients tested, exhibited a defect of α IIb β 3 integrin activation at low
279 concentrations of thrombin and convulxin (Fig. S5C), indicating a thrombopathy. Of note, the

280 expression of the main platelet receptors, glycoprotein (GP)Ib α , GPVI and α IIb β 3 integrin
281 was normal in patients, except for patient A whose α IIb β 3 level was reduced (Fig. S5D).
282 Analysis of platelet morphologies during platelet adhesion on various matrices (Fig. 2G and
283 2H and S5E) identified discoid platelets (resting stage), platelets with filopodia (intermediate
284 morphological stage), and platelets with lamellipodia or full spreading (final morphological
285 step)¹³. All patients exhibited an abnormal frequency of platelets at the final stage, except for
286 patient D2, who exhibited more resting platelets. These results indicate that the patients'
287 platelets exhibit abnormal morphological modifications during platelet adhesion and
288 spreading. Of note, platelet functional assays were also performed for two mothers. A normal
289 integrin α IIb β 3 activation was observed after stimulation of platelets by thrombin or
290 convulxin and normal platelet morphologies distributions after adhesion (Figure S6A-B).
291 Since DOCK11 is a GEF activating CDC42¹⁴, CDC42 activation was evaluated by G-LISA in
292 patients' platelets upon thrombin activation (Fig. 2I). In all tested patients (A, D1, D2, F, and
293 G), platelets exhibited impaired CDC42 activity, providing a rationale for the lower frequency
294 of filopodia stage upon adhesion and suggesting that *DOCK11* mutations are loss-of-function.
295 Predominant lamellipodia or full spreading of patient platelet suggested an impact on others
296 Rho-GTPases, such as RhoA¹⁵. In two patients tested (A and F), the RhoA activity was
297 increased (Fig. S5F). This was mimicked by pharmacological treatment of healthy donors'
298 platelets with Cdc42 inhibitor. In this condition, the RhoA activity was also increased (Fig.
299 S5F). Taken together, these results indicate an imbalance in the CDC42/RHOA activity in the
300 patients' cells.

301

302 ***DOCK11* mutated cells present abnormal morphological features**

303

304 TCR-activated T cells from patients or HDs were spread on coverslips previously coated with
305 poly-L-lysine (PLL), used as internal control, or with anti-CD28 and anti-CD3 antibodies at
306 different concentrations (Fig. 3A). On the antibodies-coated coverslips, activated T cells
307 tended to increase their spreading area along with the concentration of anti-CD3 antibody. At
308 a mild concentration (0.1 μ g/mL), patients' T cells showed reduced circularity and increased
309 area, probably as a consequence of higher numbers of protrusions formed by *DOCK11*
310 mutated T cells (Fig. S7A). At a higher anti-CD3 concentration (1 μ g/mL), mutated *DOCK11*
311 T cells had a larger spreading area than the healthy donors (Fig. 3A). Notably,
312 pharmacological activation of CDC42 restored cell spreading area to control levels (Fig. 3A).
313 These results were confirmed in activated T cells from HDs after *DOCK11* sh-RNA
314 inactivation (Fig. S7B).

315 Then, we analyzed morphologies of B-lymphoblastoid cell lines (B-LCL) after spreading on
316 anti-CD44 coated coverslips (Fig. 3B). In these conditions, some B-LCL cells from patients
317 exhibited an abnormal morphology, with numerous fine and long protrusions (Fig. 3B).

318 Finally, *DOCK11* sh-RNA inactivation was also performed in monocyte-derived dendritic
319 cells (MDDC) from healthy donors. DOCK11 expression was reduced by almost 80% at the
320 mRNA and protein levels (Fig. S7B). After activation and spreading, *DOCK11* inactivated
321 MDDC had larger and more prominent protrusions (Fig. S8A-B) and produced more IL-1 β
322 cytokine (Fig. S8C). Moreover, ruffles were aberrant and not comparable to the cells
323 transfected with the scramble sh-RNA (Fig. 3C).

324 Finally, primary skin-derived fibroblasts from patient A revealed abnormal protrusions
325 compared to healthy donor fibroblasts (Fig. S9).
326 Overall, our results suggest that DOCK11 deficiency impairs the morphology of several cell
327 lineages.

328
329

330 **DOCK11 mutations impact leukocytes migration and polarization of actin cytoskeleton** 331 **under confinement.**

332 To confirm that *DOCK11* variants impair actin cytoskeleton dynamics in lymphocytes, we
333 next compared the spontaneous migratory capacity of activated T and B-LCL cells from HDs
334 and DOCK11 patients (A to G) under confinement (Fig. 4A).

335 As previously described¹⁶, human activated HD T cells presented constant trajectories with
336 few directional changes (Fig. 4B). In contrast, all patients' derived T cells were faster than
337 their HD counterpart (Fig. 4C). Of note, patient B's mother T cells had a speed migration
338 similar to healthy donors (Figure S6C). Similarly, patient-derived B-LCL had higher
339 migration speeds (Fig. S10A). To determine whether the increased speed of DOCK11-
340 deficient cells correlated with alterations in actin polymerization, we assessed the front-rear
341 distribution of actin in T cells fixed during migration in microchannels. In agreement with
342 previous work¹⁶, HD cells presented a bimodal actin-distribution, at the front and the rear of
343 the cells (Fig. 4D). In contrast, DOCK11-deficient cells accumulated more actin at the rear of
344 the cell (i.e., reduced front/rear actin ratio) in tested patients, consistent with the increased
345 speed of these cells (Fig. 4C-D).

346 Mechanistically, the motility of activated T cells in microchannels depends on the balance in
347 actin polymerization at the front (reflecting CDC42 activity) and rear (reflecting RHOA
348 activity) of the cell¹⁷. These results were also observed in activated T cells from HDs after
349 *DOCK11* sh-RNA inactivation (Fig. S10C).

350 Considering that DOCK11 has been associated with CDC42 activation^{7,14}, we hypothesized
351 that the DOCK11 defects could reduce the activity of actin nucleators at the leading edge,
352 which would displace the balance of actin polymerization and increase polymerization at the
353 rear of the cells (thus increasing their speed). To test this hypothesis, HD T cells were treated
354 with a pharmacological RAC1/CDC42 inhibitor. This treatment increased the speed of control
355 T cells and impaired the front-rear ratio of actin polarization, recapitulating the alterations
356 displayed by the DOCK11-deficient cells (Fig. 4E, figure S10D). Altogether our results
357 suggest that DOCK11 is a critical regulator of the actin cytoskeleton dynamics and leukocytes
358 migration under confinement.

359

360 **DOCK11 deficiency results in abnormal Tregs phenotype and STAT5B activation in** 361 **lymphocytes.**

362 We next analyzed the impact of DOCK11 deficiency on the immune phenotype and some
363 immune functions. Flow cytometry immunophenotyping revealed variable alterations of
364 circulating immunoglobulins and B cell subsets, especially increased frequencies of CD21_{low}
365 and transitional B cells (Table 1 and Sup. Table1). Elevated concentrations of APRIL and
366 BAFF were found in plasma patients (Fig. S11). Elevated plasma concentrations of
367 inflammatory cytokines were also observed in most patients (Fig. S11). Mass cytometry

368 immunophenotyping on whole blood did not reveal major alterations of cell subsets except for
369 reduced proportions of early and late NK cells, mucosal-associated invariant T (MAIT) cells,
370 and memory B cells (Fig.5). Of note, CD57 expression was significantly increased in CD4+ T
371 cells and $\gamma\delta$ T cells (Fig. S12).

372 Autoimmune manifestations were prominent in all patients. In some cases, severe
373 autoimmune enteropathy, reminiscent of the clinical presentation of FOXP3 deficient patients,
374 suggested possible Tregs dysfunctions¹⁸. Tregs lymphocytes, were first analyzed using the
375 CD4⁺CD25⁺CD127_{low} surface markers. Despite a slight decrease in patient F, the proportion
376 of this subset is comparable to the controls in the two other patients tested (Fig. 6A).
377 Conversely, we observed a substantial reduction in the expression of FOXP3, and to a lesser
378 extent, of HELIOS, by analyzing intracellular staining (Fig.6B). Therefore, the proportion of
379 activated Tregs defined as CD4+ FOXP3+ HELIOS+, was lower in these patients compared
380 to controls (Fig. 6B). These results suggested that DOCK11 could be involved in the
381 regulation of FOXP3 in Tregs. Among multiple factors regulating the FOXP3 transcription,
382 STAT5B activation has been described as a main regulator of FOXP3¹⁹. Consistent with the
383 reduced FOXP3 expression in Tregs, we found a reduced activation of STAT5B in the
384 patients' T cells compared to healthy donors upon IL2 stimulation (Fig. 5C-D). In contrast we
385 observed a normal or slightly reduced IL6-dependent STAT3 activation in the patients' cells,
386 suggesting a major impact of DOCK11 deficiency on the IL2-STAT5 pathway only (Fig
387 S13C). A decreased IL2-induced STAT5B activation is also observed in B lymphocytes and
388 MAIT cells (Fig. 5C-D). More importantly, we confirmed a decreased IL2-induced STAT5B
389 activation in T cells from patients (Fig. S13A) and from healthy donors, in which we induced
390 a decrease in DOCK11 expression by knock-down (Fig. S13B). Consistently, we also
391 observed a variably reduced proliferation upon CD3 stimulation in activated T cells from five
392 patients compared to HDs (Fig. S14). Overall, these results suggest that the DOCK11
393 deficiency is associated with an impairment of the IL2-STAT5 pathway in different patients'
394 lymphocyte subsets as well as in DOCK11 knocked-down T cells from healthy donors.

395

396 **Discussion:**

397

398 We identified seven private and rare hemizygous missense mutations of *DOCK11* leading to
399 early onset autoimmune disease. Human DOCK11 deficiency has never been described so far.
400 DOCK11 is a GEF protein of the DOCK-D family. Mostly expressed in hematopoietic cells,
401 DOCK11 is suspected to impact actin cytoskeleton remodeling through CDC42 activation, an
402 important Rho-GTPase^{8,16}.

403 All *DOCK11* mutations are predicted to be deleterious, and 3D modeling suggests that they
404 could impact the stability of the protein conformation or its interactions with putative
405 partners. Accordingly, reduced DOCK11 expression was observed in patients' platelets and
406 lymphocytes. The different variants, leading to a variable protein expression, may account for
407 the variable clinical phenotypes observed in patients. Nevertheless, all tested patients showed
408 reduced CDC42 activity in platelets, highlighting the abnormal function of the *DOCK11*
409 mutants. Decreased CDC42 activity in platelets was associated with impaired platelet
410 morphology, spreading, and activation. The spreading of platelets implicates Rho-GTPases
411 such as CDC42, RAC, and RHO via integrins activation^{13,15}. Some studies suggested that

412 CDC42 is involved in platelet filopodia formation and spreading on fibrinogen²⁰. RhoA
413 activity, implicated in lamellipodia and stress fiber formation of platelets, was increased in the
414 patients tested and increased after inhibition of Cdc42 in healthy donors' platelets. Stimulated
415 platelets from patients had a higher proportion of spread platelets, with deficient filopodia
416 formation, reflecting a potentially disrupted balance between the Rho-GTPases Cdc42 and
417 RhoA.

418 Of note, reduced integrin α IIb β 3 activation was observed in patients' platelets upon
419 stimulation with an agonist at low concentration but not at high concentration. These results
420 are consistent with a partial impairment of CDC42 activation in patients' platelets²¹.
421 Interestingly, circulating anti- α IIb β 3 antibodies were detected in patient A, who developed
422 severe ITP with highly fluctuating platelet counts. The absence of significant bleeding
423 disorder in DOCK11 patients, with or without ITP, suggests that the hemostatic role of
424 platelets is not impacted. Platelet extensive exploration highlighted impaired actin
425 cytoskeleton, abnormal activation, and disrupted Rho-Gtpase balance in all patients tested,
426 regardless of the presence or absence of thrombocytopenia. Functional non-hemostatic
427 thrombopathy may impair the immunoregulation role of platelets as described in other
428 autoimmune diseases^{12,22,23}.

429 T and B cell development and function can be disrupted in immune-related actinopathy, as
430 previously described in other DOCK deficiencies^{24,26}. Patients' T cells and *DOCK11* knock-
431 down activated T cells from healthy controls exhibited aberrant cytoskeleton rearrangement
432 with larger spreading areas and more protrusions, which could impair migration, sensing, or
433 interactions with other immune cells^{27,28}. Indeed, migration speed under confinement was
434 increased concomitantly with an abnormal actin polymerization at the rear during migration
435 of the patients' activated T cells and DOCK11 knock-down model, a finding consistent with
436 an impaired balance in the activity of Rho-GTPases²⁹. Moreover, the pharmacological
437 inhibition of RAC/CDC42 in healthy donor-derived T cells reproduced the aberrant
438 spreading, faster migration, and impaired actin polarization, as observed in patients-derived T
439 cells. Conversely, incubating the patients' T cells with a CDC42 activator restored normal
440 spreading. Taken together, these results support the conclusion that DOCK11 deficiency
441 impairs the balance between CDC42 and RhoA activity in activated T cells, as observed in
442 platelets. Interestingly, a faster migration was also observed in patients B-LCL, indicating that
443 DOCK11 would be a general regulator of lymphocyte migration. Lastly, we observed aberrant
444 protrusions and ruffles upon reduced protein expression by the *DOCK11* knock-down in
445 MDDC from healthy donors. This is reminiscent of the role of mouse Dock11 (Zizimin2) in
446 the actin remodeling of bone marrow-derived dendritic cells³⁰. The abnormal cell shape of
447 DOCK11 inactivated MDDC, and their increased production of IL-1 β suggest that the
448 patients' dendritic could contribute to the immune dysregulation observed in patients.

449 The patients' immunological phenotyping showed an abnormal distribution of the B cell
450 subsets with increased circulating BAFF and APRIL in the patients' plasma. Impaired balance
451 of B cell populations in favor of transitional and CD21_{low} B cells with elevated cytokine levels
452 of the BAFF complex may promote autoimmunity in patients, as already described in other
453 immune disorders³¹. The Dock11 deficient mouse model (known as the Zizimin 2 knock-out,
454 the mouse counterpart of DOCK11) showed disturbed B cell subsets distribution³². But
455 surprisingly, these mice did not develop autoimmune manifestations. However, many

456 examples of genetic defects lead to very different phenotypes in humans and mice. For
457 example, *Lrba* knock-out in mice has no impact on regulating the immune response, whereas
458 *LRBA*-deficient patients present with Primary immune deficiency and a broad spectrum of
459 autoimmune manifestations^{33,34}.

460 T cell subsets' distribution was not overtly disturbed except for a reduced proportion of MAIT
461 cells. NK cell subsets were also low in patients but without obvious clinical consequences
462 such as viral infections or macrophage activation syndrome. Immunosenescence of T cells
463 was increased in patients, consistent with the immune-aging role of *DOCK11* suggested by
464 the mouse models^{30,32}. Increased pro-inflammatory Th1 and Th17 cytokines in the patients'
465 plasma, without any documented infection, suggest a possible immune dysregulation that
466 could be the cause or the consequence of the patients' autoimmune and auto-inflammatory
467 phenotypes.

468 All patients presented with various clinical phenotypes, including severe autoimmune
469 cytopenia, SLE, auto-inflammatory syndrome, or lymphoproliferation. Most patients had
470 inflammatory bowel disease (IBD), and some had various immune-related skin
471 manifestations. Importantly, none of the patients had severe or recurrent infections, and
472 vaccinal responses were normal in the two tested patients indicating an overall normal
473 humoral response.

474 The severe early-onset autoimmune enteropathy observed in some patients was reminiscent of
475 the prominent symptoms observed in *FOXP3* deficient patients, suggesting a potential Tregs
476 defect in the *DOCK11* patients¹⁸. Whereas we observed a mildly reduced proportion of Tregs
477 in one patient, we found the expected proportion of this subset in the other patients. However
478 more strikingly, we found a markedly decreased expression of *FOXP3*, the master Tregs
479 transcription factor, and *HELIOS* to a lesser extent. These two transcription factors are
480 essential to sustain the Tregs suppressive functions^{35,36}. Moreover, Tregs are highly dependent
481 of *IL2* and its downstream signaling pathway, as observed in *IL2*, *IL2R*, and *STAT5B*
482 deficiencies^{37,38}, all characterized by impaired Tregs function and overt autoimmune
483 manifestations. Interestingly, we observed a reduced *STAT5B* activation in the patients' T
484 and B cells upon *IL2* stimulation. This was corroborated by a slight but consistent reduction
485 in T cell proliferation. More importantly, the reduced *IL2*-induced *STAT5B* activation is
486 observed in *DOCK11* knock-down T cells from healthy controls. All these results point to a
487 global *IL2*-*STAT5* signaling impairment in the context of *DOCK11* deficiency and provide a
488 molecular basis for the underlying mechanisms leading to autoimmunity in the patients.

489 One challenging observation is that *DOCK11* patients develop overt autoimmune
490 manifestations but not viral, bacterial, or fungal infections, whereas *DOCK8* patients
491 predominantly suffer from recurrent sinopulmonary and mucocutaneous infections, severe
492 allergy with elevated serum levels of IgE but mild or any autoimmune symptoms³⁹.
493 Nevertheless, both defects are leading to a reduced *CDC42* activity⁴⁰, which therefore seems
494 to be the main cause of the loss of cell shape integrity and abnormal motility, and indicates
495 that both GEFs are non-redundant and possibly working in concert in this process. This also
496 indicates that the impaired *CDC42* activation is not fully involved in the pathophysiological
497 mechanisms of each defect. The list of *DOCK* partners is probably far from being wholly
498 defined. Since *DOCK8* and *DOCK11* belong to different *DOCK* subfamilies, one can
499 anticipate that they may share common but also different partners. In addition, their respective

500 expression may differ according to immune cell subsets. In humans, it was reported that the
501 DOCK8 deficiency is associated with a reduced STAT3 activation in various lymphocyte
502 subsets, consistent with the observation that DOCK8 deficient patients share common clinical
503 and biological features with STAT3 deficient ones such as hyper IgE, food allergy, and
504 mucocutaneous infections related to impaired Th17 function⁴¹. In this study, we uncovered an
505 IL2-STAT5 (but not an IL6-STAT3) signalization defect and an abnormal Tregs phenotype,
506 two findings consistent with the development of autoimmunity. Surprisingly a similar Tregs
507 dysfunction has also been described in DOCK8 deficient patients, despite the lack of
508 prominent autoimmunity, further blurring the understanding of the mechanisms involved⁴².
509 Very interestingly, whereas Dock8 deficient mice have impaired Tregs function but do not
510 develop autoimmunity, Treg-specific Dock8 deficient mice have lymphoproliferation,
511 autoantibodies production, and enteropathy⁴³, thus suggesting that DOCK8 deficiency in
512 conventional T cells, or maybe in other immune subsets, is protecting from the onset of
513 autoimmunity in patients.

514 On the other hand, one might speculate that the impairment of some immune subsets, such as
515 the MAIT cells, for instance, or that the platelets abnormalities observed in the DOCK11
516 deficient patients could contribute to the development of autoimmunity. Lastly, the DOCK11
517 expression pattern is not restricted to the hematopoietic compartment but also allows its
518 expression in various skin and intestinal cells⁴⁴. Accordingly, we observed aberrant
519 protrusions of primary skin fibroblasts derived from patient A, suggesting an impact on the
520 actin cytoskeleton remodeling in non-hematopoietic cells. Therefore, it is not excluded that
521 the DOCK11 deficiency in non-hematopoietic cells contributes to tissue inflammation,
522 possibly driving the autoimmune response to these tissues.

523 Another sharp contrast with the DOCK8 deficiency is the lack of overt viral infection despite
524 the impact of the DOCK11 deficiency on T cell migration and possibly other immune cells,
525 suggesting that DOCK11 deficient T cells could convey a normal tissue surveillance, possibly
526 in line with a normal or only slightly reduced STAT3 activation. In addition to differential
527 expression in immune cells, this might also relate to DOCK11-specific functions.
528 Recently, Ide et al. identified DOCK11 as a potential therapeutic target to prevent
529 persistent HBV infection⁴⁵. In this work, the authors suggested that DOCK11 plays a role
530 in the retrograde trafficking in the HBV infection and contributes to maintaining cccDNA. If
531 this mechanism holds for other Herpes viruses, the DOCK11 deficiency might passively
532 protect from those viral infections.

533
534 In conclusion, this study describes a new X-linked immune-related actinopathy in eight
535 patients with severe early-onset autoimmunity, including SLE, caused by *DOCK11*
536 hemizygous mutations. Platelets, T, and B cells from DOCK11 deficient patients showed
537 aberrant cytoskeleton remodeling with impaired CDC42 activity. [The regulation of Foxp3 in Tregs is impaired, involving the IL2-STAT5B pathway](#). Our results underscore the crucial
538 DOCK11 function in hematopoietic cells and provide a novel example of the implication of
539 actin cytoskeleton in human immune disorders. Further analyses are warranted to better
540 understand the complex interactions between DOCK11 with other DOCK molecules, notably
541 DOCK8, as well as to better characterize the molecular link with the IL2-STAT5B pathway.
542 This can provide key information to help clinicians to adopt the best therapeutic options. All
543

544 patients have been treated with different immunosuppressive drugs that variably controlled
545 the autoimmune manifestations. Considering that the DOCK11 deficiency is impacting the
546 cell shape, the mechanical migration or the adhesion of circulating cells, T regulators and
547 possible tissue-resident immune cells, allogenic hematopoietic stem cell (HSCs)
548 transplantation could be contemplated as a therapeutic option.

549 Limits of the study: all patients present with autoimmune features that may reflect biased
550 recruitment in our laboratory. Furthermore, the identified mutations seem to confer a partial
551 DOCK11 defect. Therefore, we do not exclude that *DOCK11* mutations could be associated
552 with a broader or more severe clinical phenotype, including autoinflammatory diseases^{40,41,42},
553 or combined immune deficiencies, notably in patients with a complete DOCK11 deficiency.

554

555

556

557 **Acknowledgments, funding, and disclosures:**

558

559 We sincerely thank the patients and their families for participating in the study.

560 We thank Noémie Paillon and Dr Juan-Jose Saez-Pons from the laboratory of Dr Claire
561 Hivroz at Institute Curie, Université PSL, U932 INSERM, Integrative Analysis of T cell
562 Activation Team, Paris, France for the help with T cell spreading assay. We thank the CIQLE
563 Centre d’Imagerie Quantitative Lyon-Est (France) for expert technical assistance with the
564 electron microscopy studies. We thank Dr Dominique Lasne and Pr Delphine Borgel at
565 Necker Children’s Hospital (Hematology Department, Paris) for their assistance with platelet
566 studies.

567 We thank the staff from the *Imagine* genomic, bioinformatics and cytometry core facility and
568 the Salpêtrière CyPS cytometry facility for advice and technical assistance. Lastly, we thank
569 the attending physicians for their support and for coordinating the patients’ clinical care and
570 sample collection.

571 The study was funded by the Institut National de la Santé et de la Recherche Médicale
572 (INSERM), the French government (managed by French National Research Agency (Agence
573 Nationale de la Recherche) through the “Investissements d’avenir” program (Institut
574 Hospitalo-Universitaire Imagine, grant reference: ANR-10-IAHU-01; Recherche Hospitalo-
575 Universitaire, grant reference: ANR-18-RHUS-0010)), and other grants from the Agence
576 National de la Recherche (ANR-18-CE17-0001 “Action”, ANR-18-CE15-0017), the
577 Fondation pour la Recherche Médicale (grant reference: Equipe FRM EQU202103012670).
578 The authors acknowledge the Centre de Référence Déficits Immunitaires Héritaires
579 (CEREDIH), and the Centre de Référence des cytopénies auto-immunes de l’enfant
580 (CEREVANCE) which allowed patients enrolment through the OBS’CEREVANCE and
581 ACTION cohorts.

582 This work was also supported by several grants. C.B. was a recipient of an INSERM “poste
583 d’accueil” program and was awarded the Société Française de Pédiatrie prize. L.D. received a
584 grant from the Imagine Thesis Award program. Q.R. received an Institut Imagine MD-PhD
585 fellowship (funded by the Fondation Bettencourt Schueller) and a Société Nationale Française
586 de Médecine Interne (SNFMI) fellowship.

587 The graphical abstract was created with BioRender.com.

588

589 **Authorship contributions**

590 Conceptualization, C.B., L.D., T.G., A.F., A.K., F.A., F.E.S., I.C, F.R-L.; Methodology, I.C.,
591 P.V.; Investigation, C.B., LD., T.G., A.K., M.B., C.Bru., B.D, M.M.-N., J.S., C.R., J-C.B.,
592 P.P., M-C.S., O.P., A.M., V.P., P.V., S.B., A.V., M.Z., C.M., M.R.; Data Curation, L.D, N.G.,
593 I.C., Q.R. C.M.; Formal Analysis, C.B., L.D., I.C., T.G., P.P., Q.R.; Writing – Original Draft,
594 C.B., L.D., T.G, F.E.S., I.C., A.K, F.A., F.R-L.; Writing, Review & Editing, I.C., Q.R., N.A.,
595 P.D.A., M.C., P.P., N.C-B., F.C-H., S.F., P.D., L.L., D.M., P.R., A.W-M., M.R., B.N., J-C.B.,
596 A.M., A.K., F.A., M.B., M-C.S., C.B., L.D., F.R-L.; Visualization, I.C., L.D., C.B., Q.R.,
597 N.G., T.G., P.P., F.A., A.K., M.M-N, B.D., J-C.B., T.G.; Resources, C.L., N.A., P.D.A., B.B-
598 M., S.B-J., A.B., J.B., E.B., D.B., C.Bod., M.C., M.J., N.C-B., F.C-H., A.D., S.F., P.D., M.H.,
599 J.L-P., L.L., P.R., F.R., M.T., A.W-M., M.R., C.P., B.N.; Supervision, M.M., F.E.S., A.K.,
600 F.A., F.R-L.; Funding Acquisition, F.E.S., F.R-L.

601

602 All authors reviewed the manuscript.

603

604 **Disclosure of Conflicts of Interest**

605 L.D. is a former employee of Sanofi, France and may hold shares and/or stock options in the
606 company. Other authors have nothing to disclose.

607

608 **References**

- 609 1. Kamnev A, Lacouture C, Fusaro M, Dupré L. Molecular Tuning of Actin Dynamics in
610 Leukocyte Migration as Revealed by Immune-Related Actinopathies. *Front Immunol*
611 2021;12:750537.
- 612 2. Mastrogiovanni M, Juzans M, Alcover A, Di Bartolo V. Coordinating Cytoskeleton
613 and Molecular Traffic in T Cell Migration, Activation, and Effector Functions. *Front Cell Dev*
614 *Biol* 2020;8:591348.
- 615 3. Hodge RG, Ridley AJ. Regulating Rho GTPases and their regulators. *Nat Rev Mol*
616 *Cell Biol* 2016;17(8):496–510.
- 617 4. El Masri R, Delon J. RHO GTPases: from new partners to complex immune
618 syndromes. *Nat Rev Immunol* 2021;21(8):499–513.
- 619 5. Lougaris V, Baronio M, Gazzurelli L, Benvenuto A, Plebani A. RAC2 and primary
620 human immune deficiencies. *Journal of Leukocyte Biology* 2020;108(2):687–96.
- 621 6. Su HC, Orange JS. The Growing Spectrum of Human Diseases Caused by
622 Inherited CDC42 Mutations. *J Clin Immunol* 2020;40(4):551–3.
- 623 7. Chen Y, Chen Y, Yin W, et al. The regulation of DOCK family proteins on T and B
624 cells. *Journal of Leukocyte Biology* 2021;109(2):383–94.
- 625 8. Dobbs K, Domínguez Conde C, Zhang S-Y, et al. Inherited DOCK2 Deficiency in
626 Patients with Early-Onset Invasive Infections. *N Engl J Med* 2015;372(25):2409–22.
- 627 9. Engelhardt KR, Gertz EM, Keles S, et al. The extended clinical phenotype of 64
628 patients with DOCK8 deficiency. *J Allergy Clin Immunol* 2015;136(2):402–12.
- 629 10. Kunitzura K, Uruno T, Fukui Y. DOCK family proteins: key players in immune
630 surveillance mechanisms. *International Immunology* 2020;32(1):5–15.
- 631 11. Tunyasuvunakool K, Adler J, Wu Z, et al. Highly accurate protein structure prediction
632 for the human proteome. *Nature* 2021;596(7873):590–6.
- 633 12. Linge P, Fortin PR, Lood C, Bengtsson AA, Boilard E. The non-haemostatic role of
634 platelets in systemic lupus erythematosus. *Nat Rev Rheumatol* 2018;14(4):195–213.

- 635 13. Aslan JE, McCarty OJT. Rho GTPases in platelet function. *J Thromb Haemost*
636 2013;11(1):35–46.
- 637 14. Lin Q, Yang W, Baird D, Feng Q, Cerione RA. Identification of a DOCK180-related
638 Guanine Nucleotide Exchange Factor That Is Capable of Mediating a Positive Feedback
639 Activation of Cdc42*. *Journal of Biological Chemistry* 2006;281(46):35253–62.
- 640 15. Goggs R, Williams CM, Mellor H, Poole AW. Platelet Rho GTPases—a focus on novel
641 players, roles and relationships. *Biochem J* 2015;466(3):431–42.
- 642 16. Gajardo T, Lô M, Bernard M, et al. Actin dynamics regulation by TTC7A/PI4KIII α
643 axis limits DNA damage and cell death during leukocyte migration [Internet]. *Immunology*;
644 2021 [cited 2022 Jul 19]. Available from:
645 <http://biorxiv.org/lookup/doi/10.1101/2021.10.14.464382>
- 646 17. Mack NA, Georgiou M. The interdependence of the Rho GTPases and apicobasal cell
647 polarity. *Small GTPases* 2014;5(2):10.
- 648 18. Park JH, Lee KH, Jeon B, et al. Immune dysregulation, polyendocrinopathy,
649 enteropathy, X-linked (IPEX) syndrome: A systematic review. *Autoimmun Rev*
650 2020;19(6):102526.
- 651 19. Burchill MA, Yang J, Vogtenhuber C, Blazar BR, Farrar MA. IL-2 receptor beta-
652 dependent STAT5 activation is required for the development of Foxp3+ regulatory T cells. *J*
653 *Immunol* 2007;178(1):280–90.
- 654 20. Pleines I, Eckly A, Elvers M, et al. Multiple alterations of platelet functions dominated
655 by increased secretion in mice lacking Cdc42 in platelets. *Blood* 2010;115(16):3364–73.
- 656 21. Pula G, Poole AW. Critical roles for the actin cytoskeleton and cdc42 in regulating
657 platelet integrin $\alpha 2\beta 1$. *Platelets* 2008;19(3):199–210.
- 658 22. Nelson VS, Jolink A-TC, Amini SN, et al. Platelets in ITP: Victims in Charge of Their
659 Own Fate? *Cells* 2021;10(11):3235.
- 660 23. Boilard E, Blanco P, Nigrovic PA. Platelets: active players in the pathogenesis of
661 arthritis and SLE. *Nat Rev Rheumatol* 2012;8(9):534–42.
- 662 24. Dupré L, Boztug K, Pfajfer L. Actin Dynamics at the T Cell Synapse as Revealed by
663 Immune-Related Actinopathies. *Frontiers in Cell and Developmental Biology* 2021;9:1046.
- 664 25. Gadea G, Blangy A. Dock-family exchange factors in cell migration and disease.
665 *European Journal of Cell Biology* 2014;93(10–12):466–77.
- 666 26. Tangye SG, Pillay B, Randall KL, et al. Deducator of cytokinesis 8-deficient CD4+
667 T cells are biased to a TH2 effector fate at the expense of TH1 and TH17 cells. *J Allergy Clin*
668 *Immunol* 2017;139(3):933–49.
- 669 27. Moulding DA, Record J, Malinova D, Thrasher AJ. Actin cytoskeletal defects in
670 immunodeficiency. *Immunol Rev* 2013;256(1):282–99.
- 671 28. Papa R, Penco F, Volpi S, Gattorno M. Actin Remodeling Defects Leading to
672 Autoinflammation and Immune Dysregulation. *Front Immunol* 2021;11:604206.
- 673 29. Ridley AJ. Rho GTPase signalling in cell migration. *Curr Opin Cell Biol*
674 2015;36:103–12.
- 675 30. Sakabe I, Asai A, Iijima J, Maruyama M. Age-related guanine nucleotide exchange
676 factor, mouse Zizimin2, induces filopodia in bone marrow-derived dendritic cells. *Immun*
677 *Ageing* 2012;9:2.
- 678 31. Ma K, Du W, Wang X, et al. Multiple Functions of B Cells in the Pathogenesis of
679 Systemic Lupus Erythematosus. *Int J Mol Sci* 2019;20(23):E6021.
- 680 32. Matsuda T, Yanase S, Takaoka A, Maruyama M. The immunosenescence-related gene
681 Zizimin2 is associated with early bone marrow B cell development and marginal zone B cell
682 formation. *Immun Ageing* 2015;12:1.

- 683 33. Tesch VK, Abolhassani H, Shadur B, et al. Long-term outcome of LRBA deficiency
684 in 76 patients after various treatment modalities as evaluated by the immune deficiency and
685 dysregulation activity (IDDA) score. *J Allergy Clin Immunol* 2020;145(5):1452–63.
- 686 34. Gámez-Díaz L, Neumann J, Jäger F, et al. Immunological phenotype of the murine
687 *Lrba* knockout. *Immunol Cell Biol* 2017;95(9):789–802.
- 688 35. Wing JB, Tanaka A, Sakaguchi S. Human FOXP3+ Regulatory T Cell Heterogeneity
689 and Function in Autoimmunity and Cancer. *Immunity* 2019;50(2):302–16.
- 690 36. Kim H-J, Barnitz RA, Kreslavsky T, et al. Stable inhibitory activity of regulatory T
691 cells requires the transcription factor Helios. *Science* 2015;350(6258):334–9.
- 692 37. Chinen T, Kannan AK, Levine AG, et al. An essential role for the IL-2 receptor in
693 Treg cell function. *Nat Immunol* 2016;17(11):1322–33.
- 694 38. Kanai T, Jenks J, nadeau K. The STAT5b Pathway Defect and Autoimmunity.
695 *Frontiers in Immunology* [Internet] 2012 [cited 2023 Feb 24];3. Available from:
696 <https://www.frontiersin.org/articles/10.3389/fimmu.2012.00234>
- 697 39. Su HC. Insights into the pathogenesis of allergic disease from dedicator of cytokinesis
698 8 deficiency. *Curr Opin Immunol* 2023;80:102277.
- 699 40. Harada Y, Tanaka Y, Terasawa M, et al. DOCK8 is a Cdc42 activator critical for
700 interstitial dendritic cell migration during immune responses. *Blood* 2012;119(19):4451–61.
- 701 41. Keles S, Charbonnier LM, Kabaleeswaran V, et al. DOCK8 Regulates STAT3
702 Activation and Promotes Th17 Cell Differentiation. *J Allergy Clin Immunol*
703 2016;138(5):1384-1394.e2.
- 704 42. Janssen E, Morbach H, Ullas S, et al. Dedicator of cytokinesis 8-deficient patients
705 have a breakdown in peripheral B-cell tolerance and defective regulatory T cells. *J Allergy*
706 *Clin Immunol* 2014;134(6):1365–74.
- 707 43. Janssen E, Kumari S, Tohme M, et al. DOCK8 enforces immunological tolerance by
708 promoting IL-2 signaling and immune synapse formation in Tregs. *JCI Insight* 2(19):e94298.
- 709 44. Uhlen M, Oksvold P, Fagerberg L, et al. Towards a knowledge-based Human Protein
710 Atlas. *Nat Biotechnol* 2010;28(12):1248–50.
- 711 45. Ide M, Tabata N, Yonemura Y, et al. Guanine nucleotide exchange factor DOCK11-
712 binding peptide fused with a single chain antibody inhibits hepatitis B virus infection and
713 replication. *Journal of Biological Chemistry* [Internet] 2022 [cited 2023 Feb 18];298(7).
714 Available from: [https://www.jbc.org/article/S0021-9258\(22\)00538-5/abstract](https://www.jbc.org/article/S0021-9258(22)00538-5/abstract)
715

Table 1. Clinical and biological data of the cohort															
Patients	Patient A		Patient B		Patient C		Patient D1	Patient D2		Patient E		Patient F		Patient G	
AA change	p.L1298R		p.H1336R		p.T275S		p.D414Y	p.D414Y		p.L1706S		p.R1366Q		p.R1885C	
Age (year)	14		7		29		20	20		20		6.5		14	
Clinical manifestations															
Age at onset (year)	1.4		5		5		14	9		3		5		5	
Autoimmune manifestations	Severe ITP		RF Polyarticular JIA		Evans		SLE	SLE		Evans		AI neutropenia		Evans	
Skin manifestation	Sweet syndrome, panniculitis		-		Folliculitis		Oral discoid LE	Bullous cutaneous SLE		-		Ecthyma gangrenosum		-	
Digestive manifestation	Severe IBD (ileo-colitis)		Colon Cryptitis		-		Ileitis	-		-		Anal and oral ulcers Intermittent diarrhea		-	
Others	Non regenerative anemia		Hemolytic anemia		-		PID, Growth retardation	Growth retardation		-		Auto-inflammatory syndrome, Lymphoproliferation, underweight		-	
Therapies	Corticosteroids, IVIG, rituximab, azathioprine, everolimus, infliximab		Corticosteroids, methotrexate, adalimumab		Corticosteroids		Corticosteroid, MMF, HCQ, belimumab	Steroids, HCQ		IVIG, corticosteroids		Antibiotics		Corticosteroids, Rituximab, sirolimus	
Immunophenotype	Defect memory and transitional B cells		Normal B cells, T and NK lymphopenia, NC		Excess of CD21 _{low} B cells, B cell lymphopenia, diminished MZB and switched memory B cells		Excess CD21 _{low} and transitional B cells, diminished MZB	Excess CD21 _{low} and transitional B cells, NK lymphopenia		Normal, NC		Global lymphopenia, excess of CD21 _{low} and transitional B cells		Diminished switch memory B cells and excess of transitional B cells	
Immunoglobulin dosage	Value	Reference values	Value	Reference values	Value	Reference values	Value	Value	Reference values	Value	Reference values	Value	Reference values	Value	Reference values
gr/L	IgG 14 IgA 2.15 IgM 0.25	6.6-15.3 0.5-2.2 0.53-1.62	IgG N IgA N IgM N	-	IgG 1.24 IgA <0.05 IgM 0.46	6.6-15.3 0.5-2.2 0.53-1.62	γ 26.3 g/L	γ 17 gr/L	6.9-15	IgG 10.73 IgA 1.24 IgM 0.42	6.44-11.96 0.63-2.02 0.416-1.31	IgG 27 IgA 3 IgM 7	5.5-11.15 0.4-1.6 0.5-1.5	IgG 3.69 IgA 0.16 IgM 0.25	6.6-15.3 0.5-2.2 0.53-1.62
Autoantibodies	ANCA, anti-αIIbβ3, ANA, anti-TPO, anti-thyroglobulin		RF, +IgG Coombs		+ IgG Coombs		ANA, RF, anti-RNP, anti-Sm	ANA, RF, anti-RNP, anti-Sm		+IgG Coombs		weak + anti-CD16		+ IgG and complement Coombs	

716 **Table 1 – Clinical and biological phenotypes of *DOCK11* mutated patients**

717 Listed are reference ranges or laboratory values for the patients' age groups. Therapy refers to
718 all therapies that patients received.

719 ITP: immune thrombocytopenia, IBD: inflammatory bowel disease, JIA: Juvenile Idiopathic
720 Arthritis, SLE: Systemic Lupus erythematosus, AI neutropenia: Autoimmune neutropenia,
721 LE: Lupus erythematosus, PID: pulmonary interstitial disease. IVIG: intravenous
722 immunoglobulins, MMF: mycophenolate mofetil, HCQ: hydroxychloroquine. NC: denotes
723 for Not complete B phenotype, MZB: marginal zone B cells ,N: normal values, γ : gamma-
724 globulins detected in serum protein electrophoresis, ANCA: anti-neutrophil cytoplasmic
725 antibody , ANA: antinuclear antibodies, Anti- α IIb β 3: antibody against Integrin alpha-
726 IIb/beta-3, TPO: Thyroid Peroxidase antibody, RF: Rheumatoid Factor, Anti-RNP: Anti-
727 Ribonucleoprotein antibody, Anti-Sm: Anti-smooth muscle antibody , + IgG Coombs:
728 positive direct Coombs with detection of IgG, + IgG and complement Coombs: positive direct
729 Coombs with detection of IgG and C3.

730

731

732 **Figure 1 - *DOCK11* hemizygous mutations: structural consequences and protein**
733 **expression:** Panel (A) shows dermatological clinical findings of *DOCK11* deficiency patients
734 (from left to right): lobular panniculitis on feet in Patient A, bullous cutaneous SLE in Patient
735 D2, non-infectious ecthyma gangrenosum on external lateral border of the right foot in Patient
736 F. (B) Schematic overview of *DOCK11* protein with the positions of patients' *DOCK11*
737 mutations. Molecular partners described to interact with *DOCK11* are mentioned below the
738 domain they bind. (C) 3D structure of human *DOCK11*, as predicted by AlphaFold2 (ribbon
739 representation, except for DRH2 which is shown as a blue surface). Confidence is high
740 (pLDDT>90) for the individual domain 3D structures, whereas the 3D structure of the N- and
741 C-terminal sequences, linkers between domains and large loops (often disordered) remain
742 elusive (low pLDDT values - asterisks). Two such very large loops are depicted with broken
743 lines, with the amino acid intervals. Positions of the domains relative to each other also
744 remain uncertain, except form the C2-DHR1 interface (very low PEA (predicted error
745 alignment) values). Mutated amino acids are depicted in magenta (Patients A, B, C, D and F).
746 D414 is predicted exposed at the surface of the C2 domain and likely to play a significant role
747 in the C2-DRH1 interface (Fig. S6A-C). L1298 is predicted with confidence as being buried
748 with the hydrophobic core of the ARM repeats, conserved in *DOCK-C* proteins (Fig. S6D).
749 The region including H1336 and R1366, more variable and predicted with a lower confidence,
750 is located at the concave surface of the ARM repeats, where interactions take place in
751 complexes of other *DOCK* proteins with partners. (D) 3D structure of DHR-2 domain of
752 human *DOCK11*, as predicted by AlphaFold2. The DHR-2 (in light blue) is represented
753 interacting with CDC42 (in gray), as deduced from the superimposition of *DOCK11* with the
754 3D structure of *DOCK9* in complex with CDC42. Mutated amino acids are depicted in
755 magenta and correspond to patients E and G mutations. L1706 is in the hydrophobic core of
756 DHR2 lobe A, important for dimerization. R1885 is part of DHR2 lobe B, which consists of
757 two sheets predicted in direct contact with the switch 1 domain of CDC42. (E) *DOCK11*
758 expression was evaluated in activated T cells of healthy donors (HDs) and patients (A, B, C,
759 D1, F and G) by Western blotting. Dotted lines indicate that the samples were derived from
760 the same gel but were non-contiguous. The graph shows the relative expression of *DOCK11*
761 versus HDs (set to 1) \pm SEM after normalization against Ku-70 expression).
762
763

764 **Figure 2 - Study of platelets from *DOCK11* mutated patients: (A)** *DOCK11* expression
765 was evaluated in platelets of healthy donors (HDs) and patients (A, C, D1, D2, F and G) by
766 Western blotting. Dotted lines indicate that the samples were derived from the same gel but
767 were non-contiguous. The graph shows the mean of the relative expression of *DOCK11*
768 versus HD (set to 1) \pm SEM after normalization against β -actin expression from several
769 independent experiments (HDs, n = 69; A, n = 22; C, n = 14; G, n = 16; D1, D2, n = 8; F, n =
770 15). Statistical difference was evaluated by one-way ANOVA with Dunnett's correction test
771 for multiple comparisons ($*p < 0.05$; $***p < 0.001$). **(B)** Platelet count for each patient (A, C,
772 D1, D2, F, G) was determined by automated blood cell counter. Shaded area represents the
773 normal range between 150×10^9 and 400×10^9 platelets/L. Patients A and C were investigated
774 for their platelet count several times (2 and 3 times, respectively). **(C)** Platelet size was
775 evaluated by flow cytometry. Each dot represents the mean size measured by the mean
776 forward scatter height (FSC-H; a.u., arbitrary units) of washed platelets from healthy donors
777 (HDs) and patients. The box-and-whisker plot shows the normal range, determined from HDs.
778 Whiskers represent the 5-95 percentiles, the box correspond to the interquartile range, the
779 center line is the median and the cross indicates the mean of 65 platelets. **(D)** Platelet
780 ultrastructure which was analyzed once for each patient using transmission electron
781 microscopy (TEM). Scale bar represents 1 μ m. **(E, F)** TEM analysis of platelet ultrastructure
782 in each patient. Platelet surface (E) and platelet shape (F) which is defined as the ratio
783 between the largest diameter and the smallest diameter are derived from the TEM images.
784 Graphs represent the mean \pm SEM of at least 1100 HD's platelets and 100 patient's platelets.
785 Statistical significance was determined in a one-way ANOVA with the Dunnett's post-test for
786 multiple comparisons. **(G)** Graph represents the mean percentage \pm SEM of discoid platelets
787 (dark grey), platelet with filopodia (light grey) and platelets with lamellipodia or full
788 spreading (white) of at least 150 analyzed platelets from several independent experiments
789 (HDs, n=17; patient A, n=4; patient C, n=3). Statistical significance was determined only for
790 patients A and C compared to HDs in a one-way ANOVA with the Dunnett's post-test for
791 multiple comparisons ($* p < 0.05$; $** p < 0.01$). Patients D1, D2, F and G were not
792 statistically analyzed since only one experiment was performed. Scale bar represents 10 μ m.
793 **(H)** Spreading of HD and patients' platelets onto fibrinogen matrix for 30 minutes was
794 analyzed by epifluorescence microscopy in the presence of apyrase (5 U/mL) and
795 indomethacin (4.5 μ M). Platelet morphology was visualized using F-actin detection by
796 fluorescently labeled-phalloidin. **(I)** CDC42 activity evaluated in HDs' platelets and patients'
797 platelets by G-LISA after stimulation by 0.5 U/mL thrombin for 1 minute in unstirred
798 conditions. Graph represents the relative CDC42 activity of each patient compared to that of
799 HD (set to 100%).
800
801

802 **Figure 3 - *DOCK11* mutations lead to abnormal cell morphologies:** Spreading assays with
803 different lymphocytes subsets. **(A)** T cell morphologies after spreading. Blue color
804 corresponds to DAPI staining (nucleus). Red color corresponds to actin staining. Each patient
805 is represented by a different symbol: Patient A (*), patient B (●), patient C (■), patient D1 (×),
806 patient D2 (★), patient F (▽), patient G (◐). Coverslips were coated with either poly-L-lysine
807 (i); poly-L-lysine, anti-CD28 and anti-CD3 (0,1µg/mL) antibodies (ii); or poly-L-lysine, anti-
808 CD28 and anti-CD3 (1µg/mL) antibodies (iii). Scale is set at 10µm. Cell area was measured
809 with or without CN02 treatment (CDC42/RAC1 activator). Non-parametric Kruskal-Wallis'
810 test was performed (* $p < 0.05$). **(B)** B-lymphoblastic cell lines morphologies after spreading.
811 Several morphologies were observed: cells with no protrusion, cells spread along one axis,
812 cells with fine protrusions (filopodia), cells with lamellipodia and cells presenting both
813 lamellipodia and filopodia. Cells patients presented abnormal protrusions. Repartition of each
814 morphology types is shown. Scale is set at 10µm. **(C)** Morphologies of mature monocyte-
815 derived dendritic cells (MDDC) from healthy donor, either using a scramble sh-RNA or a
816 *DOCK11*-sh-RNA, after stimulation with LPS 100ng/ml (Lipopolysaccharide) for 24 hours,
817 were observed using scanning electron microscopy (SEM). Scale is set at 5 µm.
818
819

820 **Figure 4 - DOCK11 is needed for human leukocytes migration under confinement:**
821 Analysis of human healthy donor (HD) and DOCK11-deficient T cell migration in
822 fibronectin-coated microchannels. Boxes include the 80% of the points and bars represent the
823 higher and lower 10% of points. **(A)** Representative montage of the change of position over
824 time of human T cell blast migrating inside microchannels of 4x 5µm with a timelapse of 2
825 min. **(B)** Representative kymograph of T cell blast from Healthy Donors (HD, top panel) and
826 DOCK11 patients (A – E, lower panels as indicated). **(C)** Mean instantaneous speed of HD
827 and DOCK11 T cell blasts migrating in 4 x 5µm microchannels. Results from n=2
828 independent experiments with each condition. Unpaired non-parametric Mann-Whitney test
829 was used to evaluate statistical significance between the mean speeds of controls and patients
830 (* $p < 0.05$; ** $p < 0.01$; *** $p < 0.001$). **(D)** Density maps representing the enrichment of
831 actin in HD and DOCK11 deficient T cells migrating in 8 x 5 µm microchannels. Cells were
832 allowed to migrate and fixed with 4% PFA to maintain the polarized morphology and stained
833 with phalloidin to visualize F-actin. The density maps were generated by averaging the signal
834 from HD n= 85, DOCK11A n=32, DOCK11D n=46 and DOCK11E n=63 cells.
835 Quantification of the signal intensity on density maps presented as front/rear ratio per cell.
836 One-way ANOVA was used to evaluate statistical significance. **(E)** Mean instantaneous speed
837 of HD and DOCK11 T cell blasts (patient G) migrating in 4 x 5µm microchannels, with or
838 without RAC inhibitor treatment. Results from n=2 independent experiment with each
839 condition. One-way ANOVA test was used to evaluate statistical significance. Unpaired non-
840 parametric Mann-Whitney test was used to evaluate statistical significance between the mean
841 speeds of controls and treated controls, patient and treated patient (* $p < 0.05$).
842
843

844 **Figure 5. Immune phenotype by mass cytometry**

845 (A) UMAP (Unifolm Manifold Approximation and Projection) of immune cell subsets
846 clusters analyzed by mass cytometry on whole blood samples from DOCK11 patients (n= 7)
847 and age-matched healthy donors (n=6). Each cluster is color coded. (B) Cell cluster biases
848 observed between DOCK11 patients and healthy donors. DOCK11 patients have a
849 significantly lower percentage of CD56_{bright} NK, late NK cells, MAIT, and memory B cells.
850 Two-tailed p-values were determined with a nonparametric Mann-Whitney test. (*) *p*-value <
851 0.05; (**) *p*-value < 0.01; (***) *p*-value < 0.005.

852

853 **Figure 6. Treg phenotype and STAT5 activation**

854 (A) FoxP3 mean fluorescence intensity on Tregs from Healthy donors (HDs) and DOCK11
855 patients. Treg are defined by CD4⁺ CD25⁺ CD127^{low} as depicted in the graph on the right
856 side of the panel. (B) Representative dotplots of CD3⁺ CD4⁺ Foxp3⁺ Helios⁺ cells from
857 healthy donors (HDs) and two DOCK11 patients. (C) Representative histograms of phospho-
858 STAT5 in T, CD25⁺ T and B cells from healthy donors and DOCK11 patients. Cells were
859 stimulated for 60 min with IL2. Results for unstimulated (NS) cells are shown with the black
860 peak. (D) Kinetics of phospho-STAT5 expression upon IL2 stimulation: unstimulated (NS),
861 15 and 60 minutes. Mean fluorescence intensity (MFI) of phospho-STAT5 in T, CD25⁺ T,
862 MAIT and B cells from healthy donors (HDs) and DOCK11 patients.

863

Figure 1: DOCK11 mutations

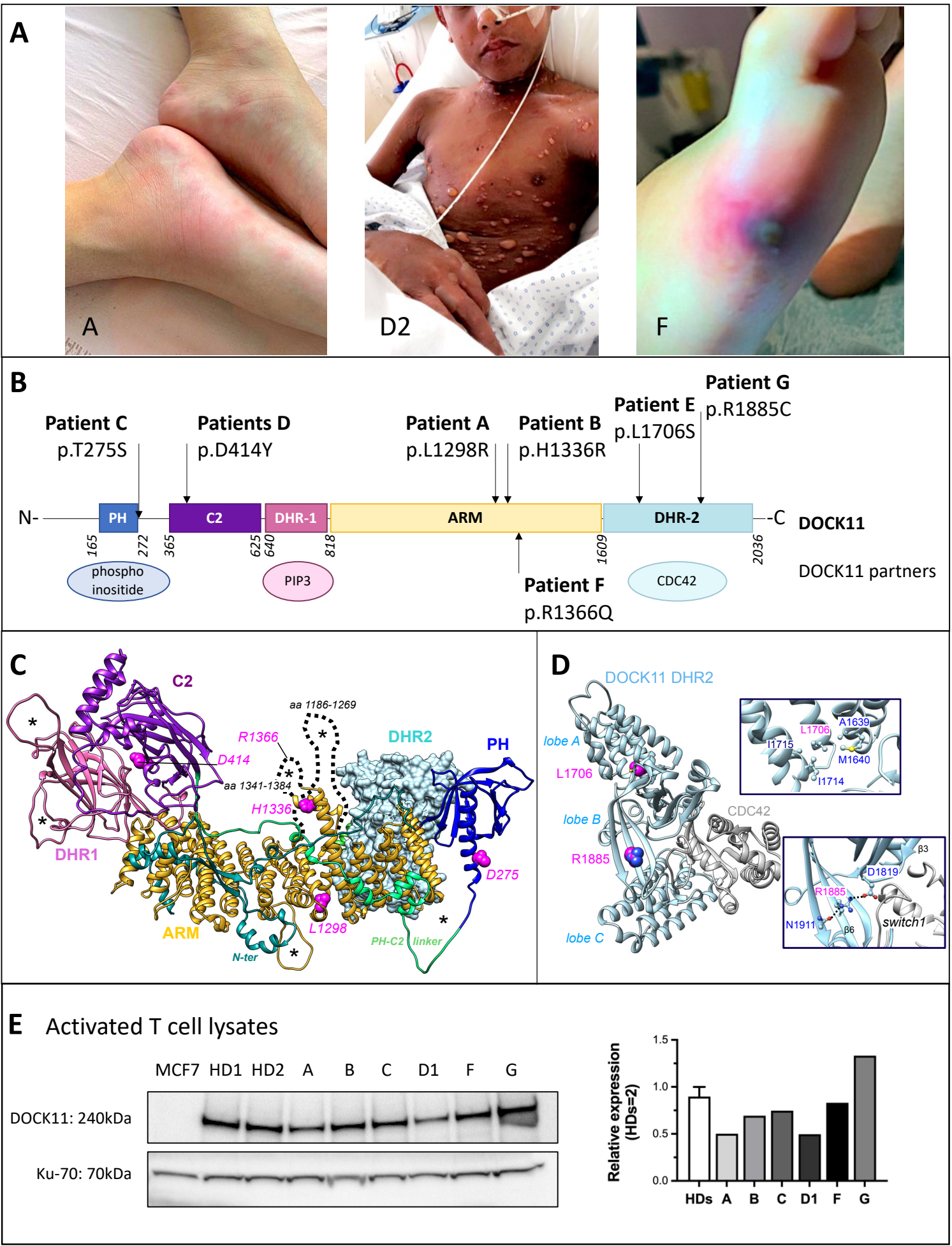


Figure 2: Platelets' study

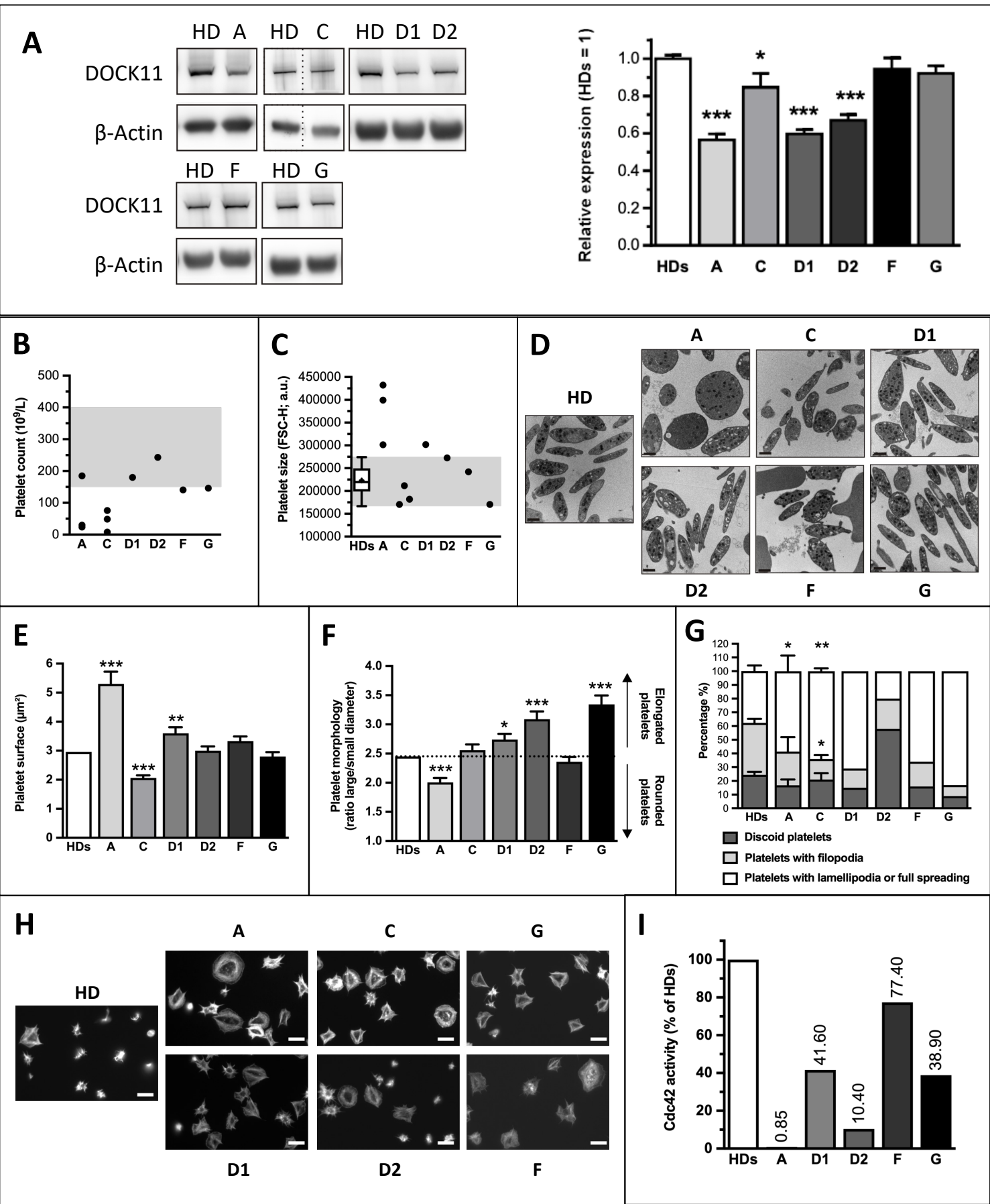


Figure 3: Morphological impairment after spreading

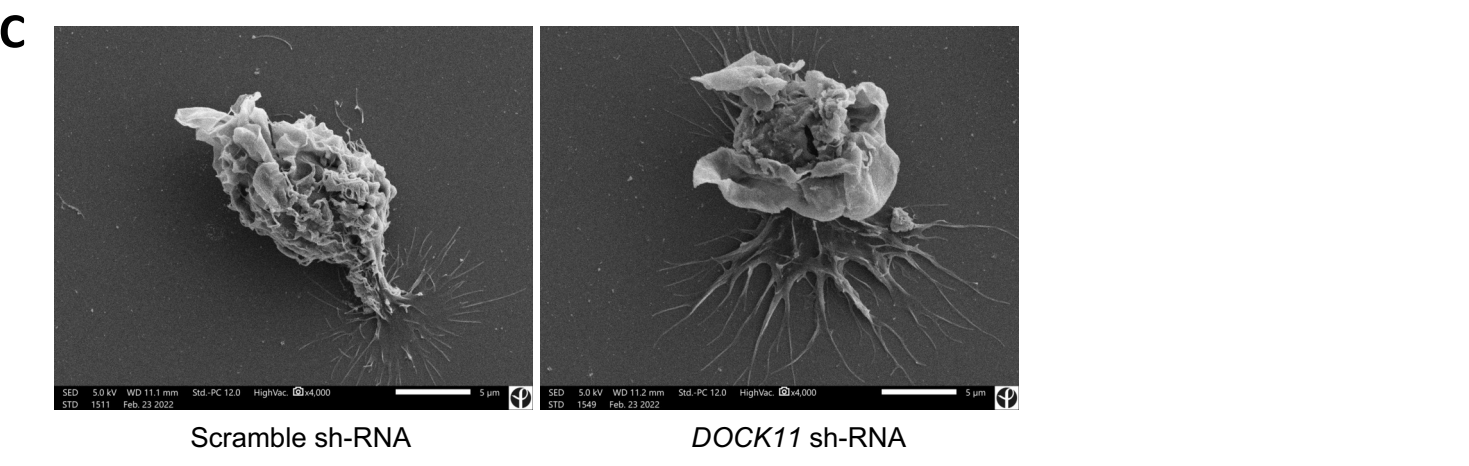
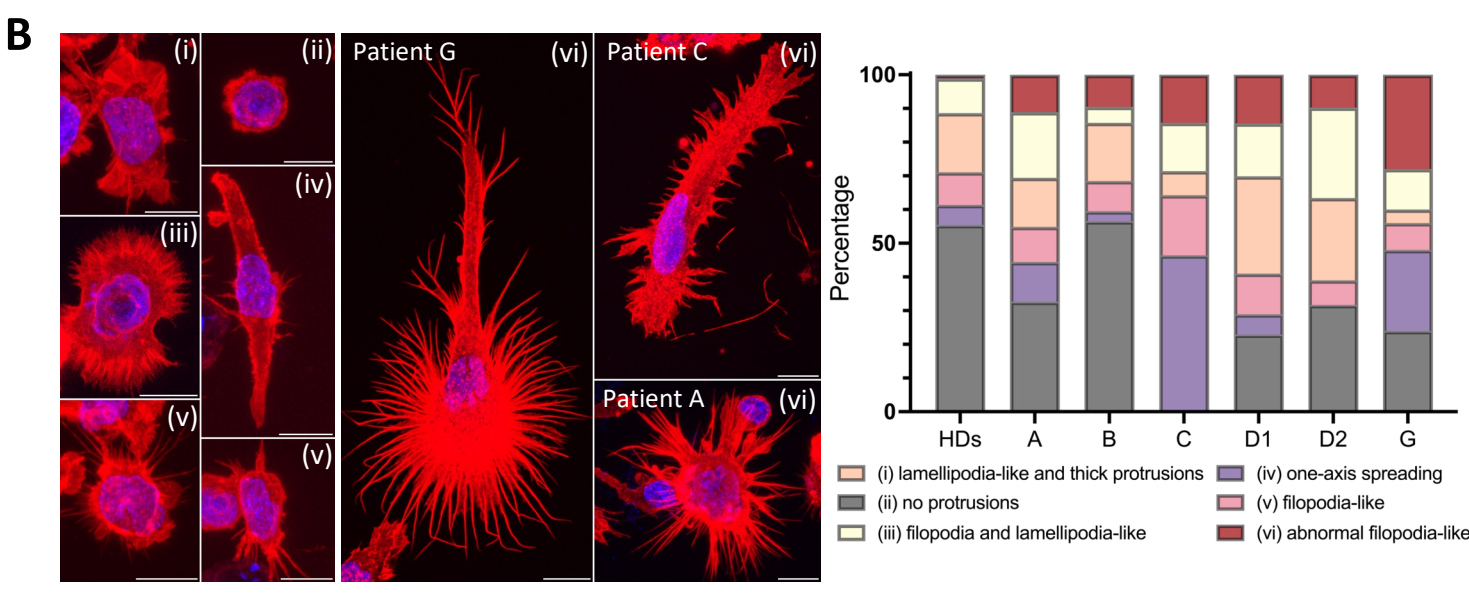
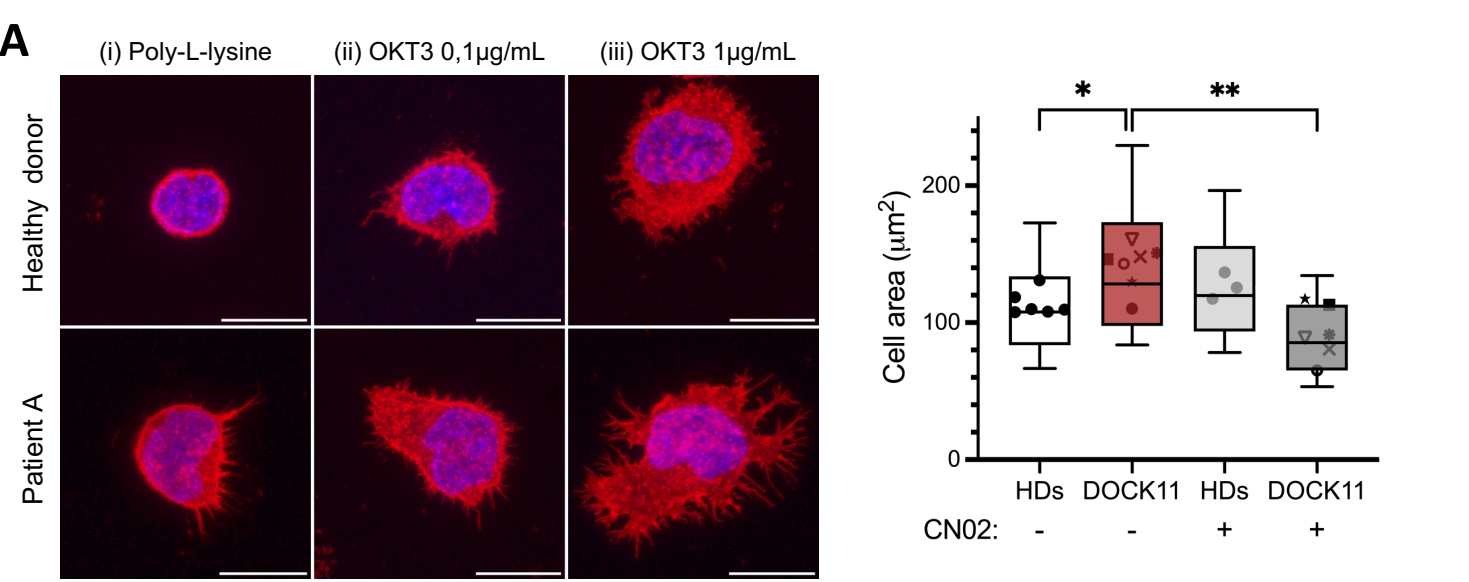


Figure 4: Migration assays – reflecting reduced CDC42 activity

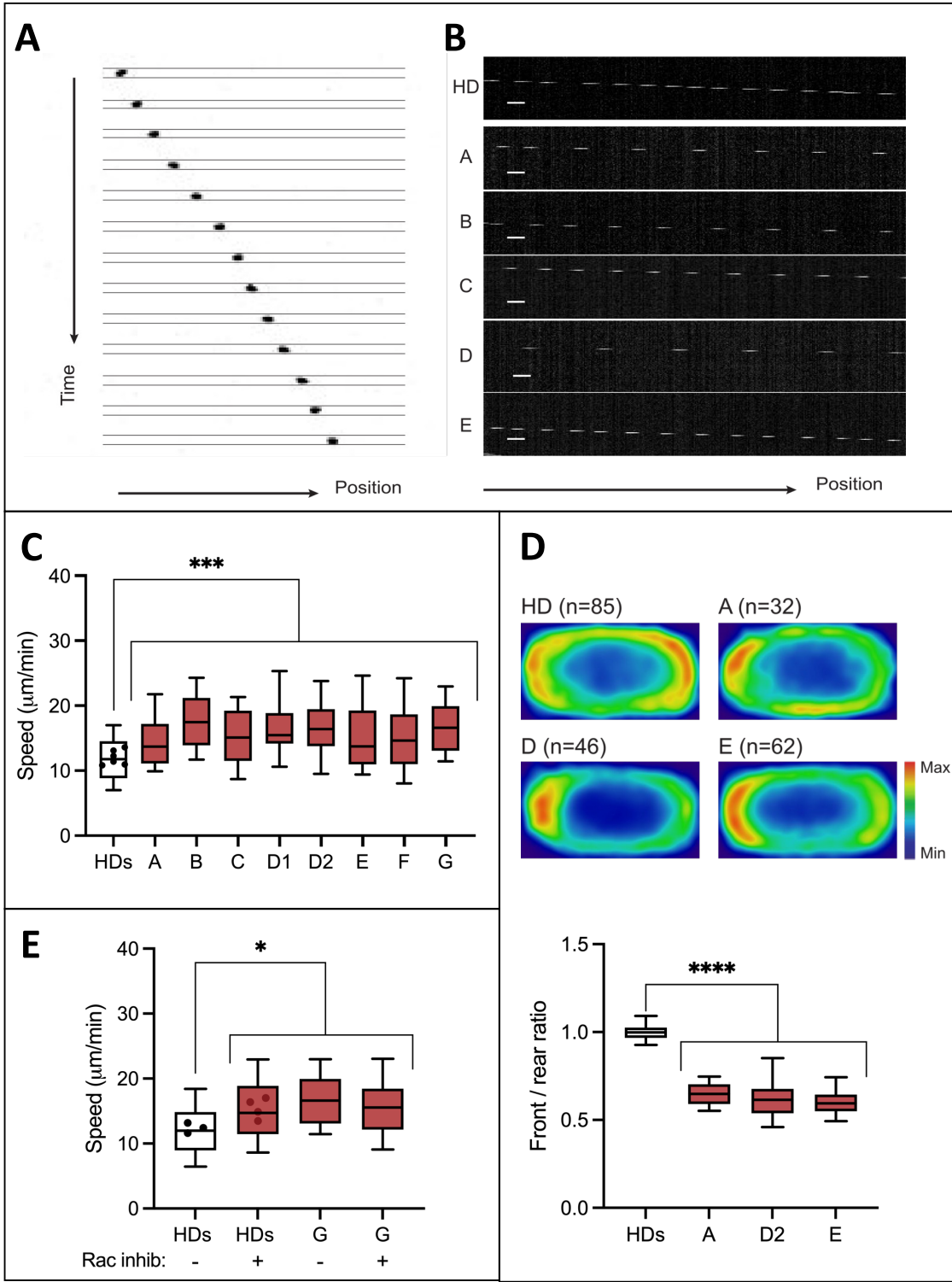


Figure 5: Immune phenotype by CyTOF

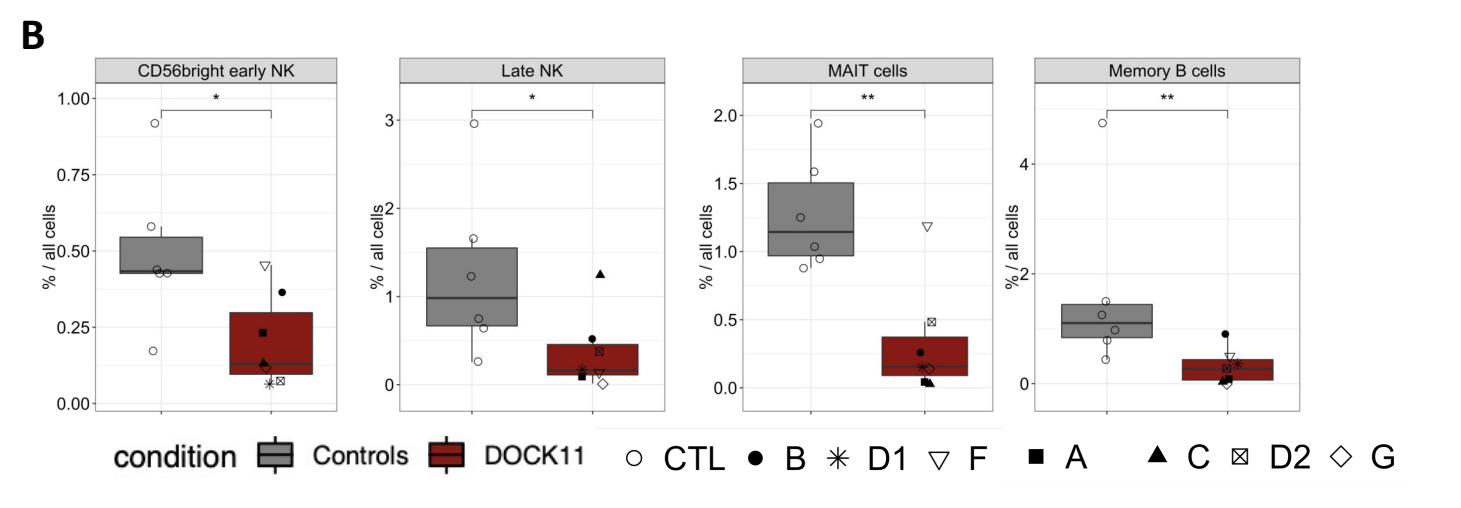
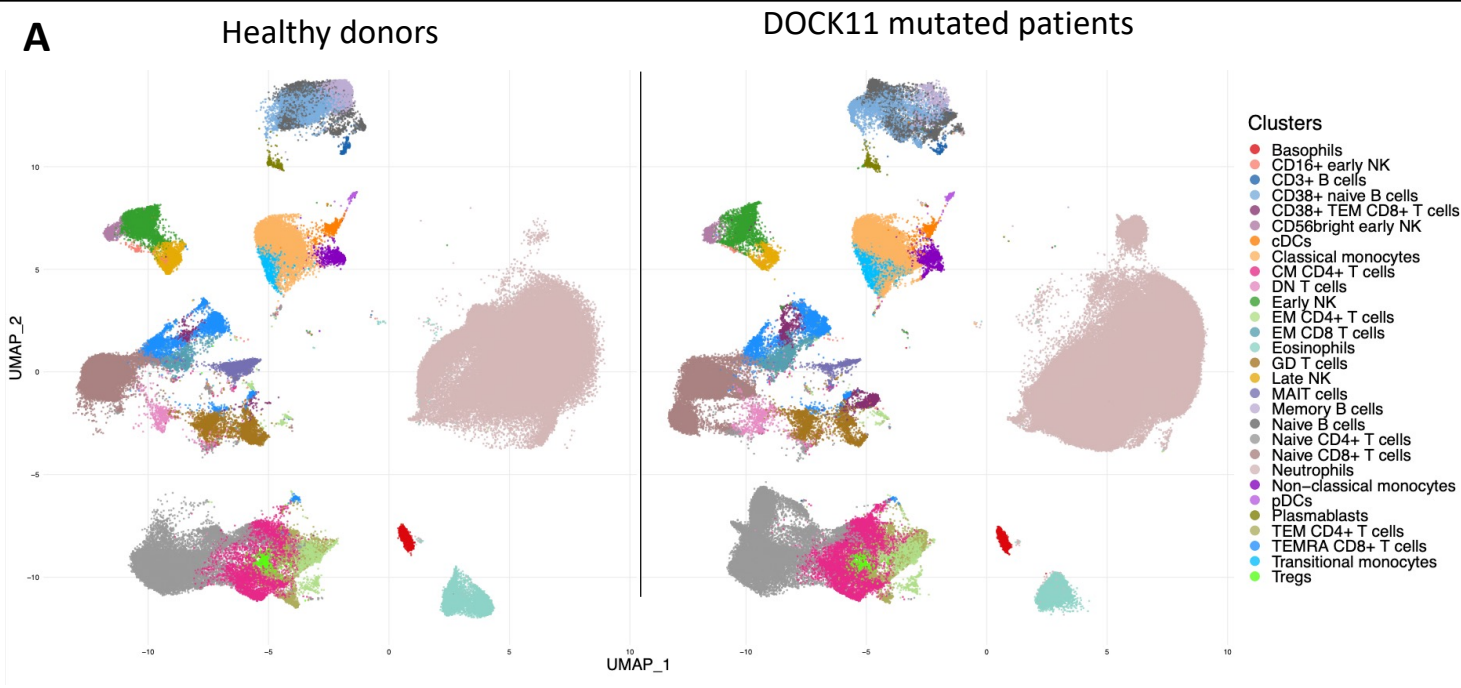


Figure 6: Treg phenotype and STAT5 activation

